Article:
Thorpe, C.L. orcid.org/0000-0002-2860-8611, Crawford, R., Hand, R.J. orcid.org/0000-0002-5556-5821 et al. (9 more authors) (2024) Microbial interactions with phosphorus containing glasses representative of vitrified radioactive waste. Journal of Hazardous Materials, 462. 132667. ISSN 0304-3894

https://doi.org/10.1016/j.jhazmat.2023.132667

Journal of Hazardous Materials 462 (2024) 132667

Contents lists available at ScienceDirect

Journal of Hazardous Materials

journal homepage: www.elsevier.com/locate/jhazmat

Research Paper

Microbial interactions with phosphorus containing glasses representative of vitrified radioactive waste

C.L. Thorpe[a,*], R. Crawford[a], R.J. Hand[a], J.T. Radford[a], C.L. Corkhill[a,e], C.I. Pearce[b], J.J. Neeway[b], A.E. Plymale[b], A.A. Kruger[d], K. Morris[c], C. Boothman[c], J.R. Lloyd[c]

[a] Immobilization Science Laboratory, Sir Robert Hadfield Building, University of Sheffield, S1 3JD, UK
[b] Pacific Northwest National Laboratory, Richland, WA, USA
[c] Williamson Research Centre and Research Centre for Radwaste Disposal, Williamson Building, University of Manchester, 176 Oxford Road, M13 9PL, UK
[d] Office of River Protection, US Department of Energy, Richland, WA, USA
[e] School of Earth Sciences, The University of Bristol, Bristol, UK

HIGHLIGHTS

- Phosphorous released from nuclear waste type glasses stimulated microbial metabolism.
- Biofilms formed on the surface of glass that contained both iron and phosphorous.
- Microbial metabolism affected the rate of glass dissolution.
- An increase in glass dissolution was associated with microbial production of volatile fatty acids.
- A decrease in glass dissolution was associated with microbial reduction of Fe(III) to Fe(II).

GRAPHICAL ABSTRACT

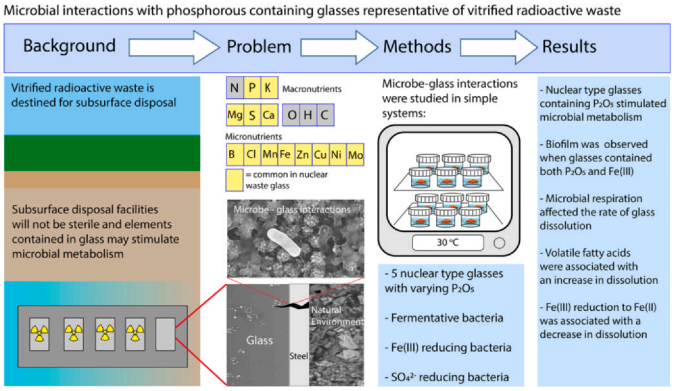

ARTICLE INFO

Editor: Shaily Mahendra

Keywords:
Nuclear waste
Biodegradation

ABSTRACT

The presence of phosphorus in borosilicate glass (at 0.1 – 1.3 mol% P_2O_5) and in iron-phosphate glass (at 53 mol % P_2O_5) stimulated the growth and metabolic activity of anaerobic bacteria in model systems. Dissolution of these phosphorus containing glasses was either inhibited or accelerated by microbial metabolic activity, depending on the solution chemistry and the glass composition. The breakdown of organic carbon to volatile fatty acids increased glass dissolution. The interaction of microbially reduced Fe(II) with phosphorus-containing glass under anoxic conditions decreased dissolution rates, whereas the interaction of Fe(III) with phosphorus-containing glass under oxic conditions increased glass dissolution. Phosphorus addition to borosilicate glasses did not significantly affect the microbial species present, however, the diversity of the microbial community was enhanced on the surface of the iron phosphate glass. Results demonstrate the potential for microbes to influence the geochemistry of radioactive waste disposal environments with implication for wasteform durability.

* Corresponding author.
E-mail address: clare.thorpe@sheffield.ac.uk (C.L. Thorpe).

https://doi.org/10.1016/j.jhazmat.2023.132667
Received 24 June 2023; Received in revised form 21 September 2023; Accepted 27 September 2023
Available online 29 September 2023

1. Introduction

Natural environments are not sterile, therefore, microorganisms must be considered when planning a deep geological disposal facility (GDF), or near surface disposal facility, for radioactive waste. The need to study microbial influence on the chemical evolution of a GDF has been acknowledged in reviews by Humphreys et al., [32], Lloyd and Cherkouk, [49], and Ruiz-Fresneda et al., [76] meanwhile, the multi-disciplinary project 'Microbiology in Nuclear Waste Disposal' (MIND), funded by the European Commission (2015–2019), targeted technical issues involving microbial processes that must be addressed to facilitate safe implementation of geological disposal. The design of radioactive waste disposal facilities varies by country, waste inventory and available geology but most are planned at depths < 1000 m (the exception being deep borehole disposal e.g. [19]) and comprise a multibarrier concept. Solid wasteforms (e.g. glass, ceramic or cement) are packaged in engineered containers (usually metal), surrounded by a buffer/backfill (usually clay or cement) and emplaced in a stable rock formation below the surface. They may contain High Level Wastes (HLW), typically heat producing spent fuel or HLW glasses, containing fission products and actinides from reprocessing. They may also contain intermediate or lower activity wastes (ILW/LLW/LAW) that are typically non-heat producing and include cementitious material, and lower activity waste glasses.

Microbial life has been observed at depths far greater than 1000 m where temperature, pore pressure and nutrients are suitable (e.g. [59,75,53,34,61,23]). In the vicinity of high level radioactive wastes microbial activity may be initially limited by temperature and radiation, however, these will decrease with time and subsurface microorganisms are adaptable to both (e.g. [48,43,79,8]). The emplacement of radioactive waste in a nutrient poor subsurface GDF will alter the surrounding biosphere, and the biosphere will, in turn, affect the evolution and degradation of the waste. The nature and function of the microbial community present in the GDF will depend on: a) the presence of water; b) the bioavailability of a carbon source (organic or inorganic); c) access to appropriate electron donors (e.g. organic carbon, H_2, Fe(II), NH_4); d) access to an appropriate electron acceptor (e.g. O_2 > NO_3^- > Mn(IV) > Fe(III) > SO_4^{2-}); and e) the availability of key macro-nutrients (e.g. N, K, P, Mg, Ca, S).

In the most nutrient limited environments, for example granites and basalts where hydrocarbons are negligible, organisms may be dormant or exist under extremely limited energy conditions at the lowest metabolic rates [36–38,85,94]. Hot spots of microbial activity can occur whenever chemical energy is available from organic or inorganic sources [18,37,62]. Chemolithoautotrophs can exist in carbon-starved subsurface environments by deriving energy from inorganic chemical reactions and fixing carbon dioxide gas to make carbon-based molecules. Hydrogen (e.g. from steel corrosion) can be consumed by bacteria in the presence of carbon dioxide and electron acceptors such as Fe(III), SO_4^{2-}, or NO_3^- to create the complex organic molecules that may support other, heterotrophic, microbial life. Such organisms have been observed during research in the Äspö Hard Rock Laboratory, a facility built to study the subsurface environment now selected for the Swedish GDF [56,64–66]. Meanwhile, another study of microbiological life found at depths of 2.8 km, concluded that radiolytically generated chemical species provided the energy and nutrients for a simple ecosystem dominated by *Candidatus Desulforudis audaxviator* [20]. The emplacement of a GDF with an engineered barrier system may create a microbial 'hot spot' generating species that stimulate an in-situ or introduced microbial community.

To date, research has focused on microbial ability to utilize organic material from ILW contained in cementitious material for example cellulose breakdown products such as isosaccharinic acid from intermediate level waste [9,44,45]. Similarly, the production of H_2 from steel corrosion, has been identified as a potential energy source for microbial life (e.g. [31,45,47,57]). Some research has shown that the clay buffer materials that surround the waste package inhibit microbial life when the water content is ≤ 15% (a_w ~0.96) [58] however these same clay materials can contain sulphate/metal reducing bacteria that could stimulate corrosion of the metal used to contain vitrified waste. In a GDF, more complex carbon sources may be available from deep groundwaters, drilling residues, superplasticisers (used in cements), nitrogen sources include N_2, NO_3^- and NH_4 [46], whilst other essential elements including, P, S, K, Ca, Mg, Cl, Fe, Cu, Co and Zn are constituents of most rock forming minerals and are also plentiful in the wasteforms themselves.

Vitrified radioactive waste, in particular, can contain most, if not all, essential metals that microorganisms require. Most are silicate or borosilicate glasses ([86] and references therein) with phosphate glass considered as an alternative but currently only produced in Russia [40,68]. Studies on microbial alteration of radioactive glass wasteforms are limited and contradictory. A study of SON68, a non-radioactive simulant of the French HLW glass, proposed that microbial biofilms have a passivating effect [5,6], whilst research into microbial degradation of natural glasses and silicate minerals demonstrated the ability of microorganisms to accelerate weathering in order to release vital nutrients (e.g. [74,89]). Accelerated weathering of vitrified material may occur through microbial production of organic acids, siderophores and other chelating compounds, or through changes to the local pH environment [63,74]. In studies of naturally occurring basaltic glass, shown to dissolve at similar rate to nuclear waste glass in model systems [84], dissolution rates were higher in the presence of microorganisms and it was hypothesised that they are able to sequester iron from the glass [63,81]. Biological weathering of glass has also been studied from the point of view of archaeological glass degradation/preservation with preferential biofouling noted on certain colours of stained glass [55,90] and some industrial processes incorporate biocides into glasses (e.g. Au or Cu) [77,93].

Despite the possibility for microbes to influence glass alteration, most glass dissolution tests are conducted under static, sterile conditions and at elevated temperatures (typically 50–200 °C) [86]. The abiotic glass corrosion processes that occur on contact with aqueous solutions or water vapour have been described at length [30]. Initially, ion exchange (between hydronium ions and alkali elements) occurs concurrent with hydrolysis of the silicon-oxygen/boron-oxygen bonds in the glass network. Then, an amorphous silicon-rich gel layer forms (either through dissolution-precipitation reactions or by reordering at the glass surface) that can crystalize over time, acting either a barrier to further dissolution, or in some cases as a driver for further dissolution [30]. In general, glass dissolution: (i) is accelerated by increasing temperature; (ii) increases with alkalinity and acidity, and (iii) is greatly influenced by solution chemistry [30].

Due to the difficulty in predicting dissolution rates even in abiotic systems, few experiments have been conducted in non-sterile environments to determine the potential influence of microbial metabolism on glass dissolution. In particular, studies are needed to link microbial metabolic processes to the chemical composition of the glass. This study focuses on phosphorus, an essential nutrient for cellular components (e.g., phospholipids, DNA, ATP) and present in several proposed nuclear waste glass compositions (e.g. [40,21,50]). Borosilicate glasses with a relatively simple chemical composition containing 0, 438, and 4380 mg kg^{-1} phosphorus were prepared and subjected to glass dissolution testing. Results were compared with tests conducted using: (i) a simulant nuclear waste glass with a more complex composition containing 5698 mg kg^{-1} phosphorus; and (ii) an iron phosphate glass containing > 200,000 mg kg^{-1} phosphorus. The phosphorus contents of these glasses span the orders of magnitude found in different rock types (Table 1).

The five glasses were exposed to microbial growth media containing three anaerobic microbial communities: fermentative, Fe(III)-reducing, and SO_4^{2-}-reducing. The aim was to ascertain a) the impact of phosphorus-containing glass on the microbial communities

Table 1
Comparison of the phosphorus content of glasses 1–5 with that of different rock types (contained mainly in the apatite mineral group). Results extracted from a larger survey by [69] and groundwater values sourced from a survey by Warrack et al., 2022.

Material	Mean concentration of phosphorus (literature data rounded to nearest 100 mg kg^{-1})
Ultramafic rock	100
Alkali Basalt	3000
Granite	500
Andesite	1000
Mudstone	1100
Sandstone	500
Siltstone	700
Average continental crust	700
Borosilicate glass 1 (0 mol% P_2O_5)	0
Borosilicate glass 2 (0.1 mol% P_2O_5)	438
Borosilicate glass 3 (1 mol% P_2O_5)	4380
Low Activity Waste glass 4 (1.3 mol% P_2O_5)	5698
Iron Phosphate glass 5 (53 mol% P_2O_5)	232297
World P concentration in groundwater	Mean < 0.1 mg L^{-1} Maximum > 750 mg L^{-1}

and b) the impact of the microbial communities on the dissolution rate of the glass.

2. Methods

2.1. Making and preparation of glasses

Six glasses were considered and five were selected for use in experiments with anaerobic microbes. Firstly, a series of borosilicate glasses, composed of seven-oxides, SiO_2, B_3O_2, CaO, Na_2O, ZrO, Al_2O_3 and P_2O_5 were made with 0, 0.1, 1 and 5 mol% P_2O_5. Melts designed to make 300 g batch of glass were prepared from reagent grade chemicals (SiO_2, $Al(OH)_3$, $CaCO_3$, $Ca_3(PO_4)_2$, H_3BO_5, Na_2CO_3 and $ZrSiO_4$) in a platinum crucible at 1270 °C (1 h unmixed and four hours stirred with a platinum paddle), annealed at 520 °C, and cooled to room temperature at 1 °C per minute. X-ray diffraction analysis (Bruker D2 Phaser with Cu Kα radiation) of borosilicate glasses containing 0, 0.1, and 1 mol% P_2O_5, revealed only diffuse scattering, confirming they were all below the solubility limit for P_2O_5, however, a crystalline Ca-Na-phosphate phase was detected in glasses containing 5 mol% P_2O_5 (SI Fig. 1). The solubility limit for P_2O_5 in this series was therefore concluded to be between 1 and 5 mol% (2–10 wt%) consistent with other borosilicate glass systems that typically contain < 7 wt% P_2O_5 before phase separation occurs [50]. Only glasses containing 0, 0.1 and 1 mol% P_2O_5 (glasses 1, 2 and 3) were used in experiments. In addition, two non-radioactive analogues of phosphorus-containing nuclear waste glasses were obtained: (1) low activity waste (LAW) LGS19 glass containing 1.3 mol% P_2O_5 (glass 4) [21]: and (2) iron phosphate glass considered for radioactive waste disposal, particularly in Russia, containing 53 mol % P_2O_5 (glass 5). The density of the glasses was determined by helium pycnometry to be 2.598 ± 0.001, 2.592 ± 0.002, 2.588 ± 0.002, 2.636 ± 0.002 and 2.935 ± 0.004 g/cm^3 for glasses 1–5 respectively (AccuPyc II 1340 pcynometer, temperature 23.89 °C, 30 purges, cell volume 1.2781 cm^3 10 repeats). All glass compositions were measured by acid digest (aqua-regia and HF) followed by inductively coupled - optical emissions spectrometry (ICP-OES) (Table 2).

2.2. Isolation of an alkali-tolerant microbial community

The microbial community used for the glass dissolution experiments must be tolerant of the alkaline conditions likely to develop in the vicinity of the glass [30]. Therefore, sediment with a pH > 8.5 was sourced from a depth of < 1 m from Harpur Hill, Derbyshire, a well characterised site with elevated pH due to historical lime-workings (e.g. [15,80]). Primary enrichment microcosms were established using a sediment inoculum (5–10% w/v) in fresh water (FW) medium (Table 3; SI Table 1), degassed with N_2 (e.g. [51]), adjusted to pH 8.5 with NaOH and with glucose as a fermentable carbon substrate. Subsequent aliquots (1% v/v) were then transferred to: a) FW medium degassed with N_2 and amended with glucose to induce fermentation; b) FW medium degassed with N_2 with Fe(III)-citrate to stimulate Fe(III)-reducing bacteria; or c) Postgate C medium (Table 3; SI Table 1) degassed with N_2 with sodium sulphate to enrich for sulphate-reducing bacteria. Glucose

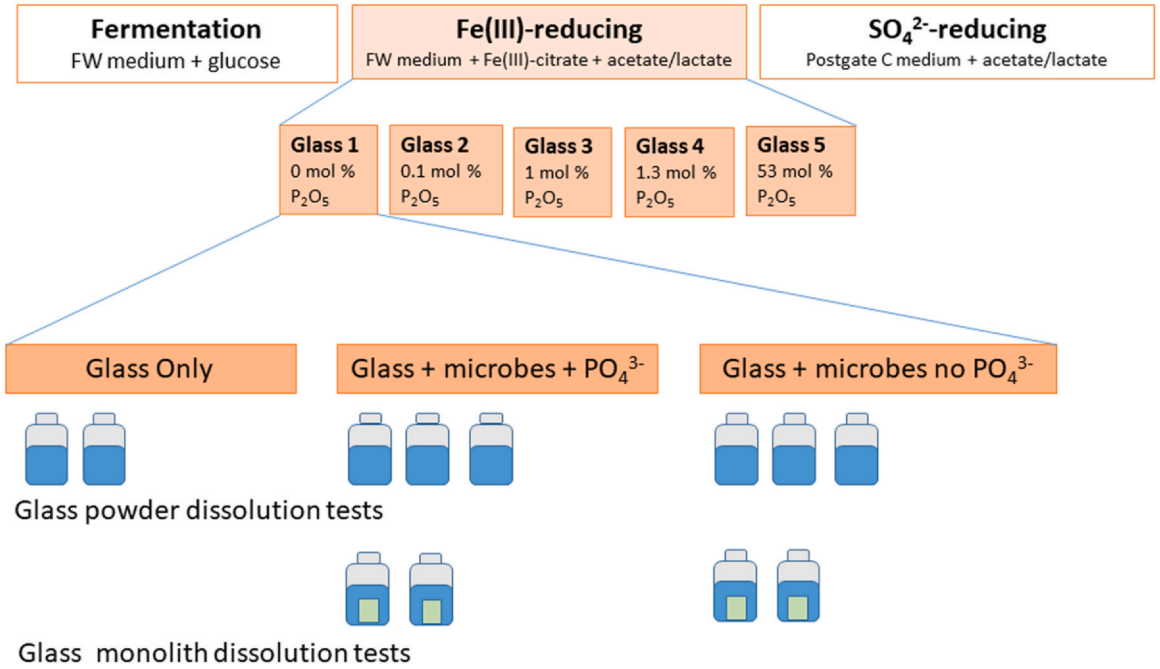

Fig. 1. Experimental matrix. Conditions and replicates are shown for glass 1 in the Fe(III)-reducing system; these conditions were repeated for all 5 glasses in all 3 systems.

Table 2
Normalised composition of glasses in weight % and mol% as determined by acid digestion and analysis by ICP-OES. The largest source of error in this process is introduced during sample digestion and is estimated at + /- 5%.

	Glass 1 Borosilicate – 0% P_2O_5		Glass 2 Borosilicate – 0.1% P_2O_5		Glass 3 Borosilicate – 1% P_2O_5		Glass 4 LAW LGS19		Glass 5 Iron phosphate glass	
	wt%	mol%	wt%	mol%	wt%	mol%	wt%	mol%	wt%	mol%
SiO_2	52.3	56.2	52.1	56.1	47.8	52.4	55.1	61.2	3.69	8.29
P_2O_5	**0.00**	**0.00**	**0.23**	**0.11**	**2.44**	**1.13**	**2.76**	**1.30**	**55.7**	**53.0**
Al_2O_3	11.6	7.38	11.6	7.37	12.4	8.01	7.82	5.12	0.48	0.64
B_2O_3	3.87	3.59	3.92	3.64	4.14	3.92	5.35	5.13	0.72	1.39
BaO									0.01	0.01
CaO	6.37	7.34	6.81	7.86	7.34	8.61	5.75	6.85	0.18	0.44
Cr_2O_3							0.14	0.06	0.02	0.02
CuO									0.02	0.03
Fe_2O_3							**0.33**	**0.14**	**35.9**	**30.4**
K_2O							1.26	0.89		
Li_2O							4.40	9.82	0.07	0.32
MgO							0.21	0.35	0.02	0.08
MnO_2									0.01	0.01
Na_2O	23.1	24.1	22.5	23.5	22.9	24.4	1.62	1.75	0.19	0.41
SrO									0.01	0.01
TiO_2							1.72	0.48	0.01	0.00
SO_3							1.73	1.45		
ZnO							0.02	0.02	2.92	4.85
ZrO_2	2.75	1.44	2.80	1.47	2.86	1.53	6.53	3.54	0.04	0.04
V_2O_5							5.30	1.94		
Total	100.00	100.00	100.00	100.00	100.00	100.00	100.00	100.00	100.00	100.00

Table 3
Fresh Water Medium components per 1 L deionised water and modified Postgate C Medium components per 1 L deionised water ([70]; Lovely and Phillips, 1986).

Component	FW media Concentration mmol L^{-1}	Postgate Concentration mmol L^{-1}
$NaHCO_3$	29.76	
Na_2SO_4		31.68
NH_4Cl	4.67	18.70
*$Na_2HPO_4{\cdot}H_2O$	3.75 or 0.31	
*KH_2PO_4		3.67
KCl	1.34	
$CaCl_2.2\,H_2O$	6.8×10^{-3}	2.80×10^{-1}
$MgSO_4.7\,H_2O$	2.9×10^{-2}	2.72×10^{-1}
$FeSO_4.7\,H_2O$	3.6×10^{-3}	1.79×10^{-2}
Nitrilotriacetic acid	7.8×10^{-2}	7.8×10^{-2}
$MnSO_4{\cdot}H_2O$	2.9×10^{-2}	2.9×10^{-2}
NaCl	1.7×10^{-2}	1.7×10^{-2}
$CoCl_2.6\,H_2O$	4.2×10^{-3}	4.2×10^{-3}
$ZnCl_2$	9.5×10^{-3}	9.5×10^{-3}
$CuSO_4.5\,H_2O$	4.0×10^{-4}	4.0×10^{-4}
$AlK(SO_4)_2.12\,H_2O$	2.1×10^{-4}	2.1×10^{-4}
* *H_3BO_3	2.1×10^{-4}	2.1×10^{-4}
Na_2MoO_4	1.21×10^{-3}	1.21×10^{-3}
$NiCl_2.6\,H_2O$	1.01×10^{-3}	1.01×10^{-3}
$Na_2WO_4.2\,H_2O$	7.58×10^{-4}	7.58×10^{-4}
Biotin	8.19×10^{-2}	8.19×10^{-2}
Folic acid	4.53×10^{-2}	4.53×10^{-2}
Pyridoxine HCl	4.86×10^{-2}	4.86×10^{-2}
Riboflavin	1.33×10^{-1}	1.33×10^{-1}
Thiamine	1.88×10^{-1}	1.88×10^{-1}
Nicotinic acid	4.06×10^{-4}	4.06×10^{-4}
Pantothenic acid	2.28×10^{-1}	2.28×10^{-1}
* **Vitamin B-12	7.38×10^{-4}	7.38×10^{-4}
p-aminobenzoic acid	3.65×10^{-1}	3.65×10^{-1}
Thioctic acid	2.42×10^{-1}	2.42×10^{-1}

*Reduced to 0.01 g in penultimate inoculation prior to addition to P_2O_5 containing glass, * * Left out of the final incubation containing glass. * **Contains ~74 μM phosphorus.

was omitted and electron donors (10 mM acetate and 15 mM lactate) were provided when Fe(III) or SO_4^{2-} were added as the sole electron acceptor (Table 4). Aliquots (1% v/v) were transferred approximately every seven days to fresh media. Fresh media were heat sterilised by autoclaving for 20 min at 126 °C and 2 bar and flushed with N_2 for 40 min per litre of liquid. The pH was then adjusted to pH 8.5 under N_2 gas before transferral to sealed glass microcosm bottles where the headspace was flushed with N_2 and incubated in the dark at 30 °C. Cultures were transferred five times until sediment carry over from the initial Harpur Hill sample was negligible.

Cells from the sixth subculture were harvested by centrifugation (20 mins at 2500 g) and washed three times in anoxic Tris(hydroxymethyl)aminomethane (TRIS) buffer pH 9 (0.96 g L^{-1} TRIS HCl and 5.32 g L^{-1} TRIS base). Cells were then re-suspended in TRIS buffer and biomass concentrations assessed by UV–vis spectrophotometry at 600 nm and diluted to a target optical density of ~ 13 (measured accurately by dilution) in a 2 mL volume, such that the addition of 50 μl to each experiment yielded an approximate final $OD_{600\,nm}$ of 0.02. This was achieved with certainty for the fermentative and SO_4^{2-}-reducing systems, however, due to interference by precipitation of Fe(II)-bearing mineral phases, cell density may be subject to analysis artefacts in the Fe(III)- reducing system. In order to exclude non-glass derived boron from the experiments, the final culture was prepared in boron free media (made without boron added to the mineral mix) and stored in bottles made from high density polyethylene (HDPE). Experiments were conducted in HDPE bottles and ICP-OES samples were acidified with ultra-pure acid stored in HDPE rather than borosilicate glass to avoid boron and silica contamination.

2.3. Glass dissolution experiments

Glasses were crushed and sieved to size fraction 75–150 μm and then washed using isopropanol to remove fine particles, according to the method described in the Product Consistency Test protocol ASTM C1285–21 [1]. In addition, monoliths were cut to dimensions ~ 15 × 15 x 5 mm and polished to 1200 grit using silicon carbide

Table 4
Summary of the three simple microbial systems.

Conditions	Media	Carbon source	Electron acceptor	Initial pH
Fermentative	FW media	Glucose (10 mM)	N/A (Fermentation)	8.5
Fe(III)-reducing	FW media	Lactate 15 mM /acetate 10 mM	Ferric citrate (55 mM)	8.5
SO_4^{2-}-reducing	Modified Postgate C	Lactate 15 mM /acetate 10 mM	$NaSO_4$ (30 mM)	8.5

(ASTM, 2021b) [2]. For each test, 1 g of crushed glass was added to each sterile HDPE vessel along with 30 mL of medium. In each system (fermentative, Fe(III)-reducing, and SO_4^{2-}-reducing), there were three variables: '**Glass only**' (no PO_4^{3-}) systems (performed in duplicate), '**Glass + microbes + PO_4^{3-}**' systems inoculated with microbes in medium containing added phosphate (performed in triplicate) and '**Glass + microbes no PO_4^{3-}**' systems where glass was inoculated with microbes in a phosphate free medium (prepared in triplicate) (Fig. 1). In parallel, duplicate monolith systems were incubated in media with and without PO_4^{3-} to image any biofilm development / microbial attachment to the glass surface, which is otherwise difficult on powdered samples. All vessels were incubated at 30 °C and agitated gently on an orbital shaker at 30 rpm to avoid clumping of the glass particles. Media were degassed and experiments inoculated in an anaerobic chamber before the vessels were sealed tightly. Ferrozine assays [83] conducted on the Fe-phosphate glass system confirmed the presence of Fe(II) in microbially active systems until at least 168 days (the longest experimental timeframe) confirming that, although some ingress of oxygen inevitably occurred, this was slow enough that solutions remained anaerobic.

Aliquots (1 mL) of the media were removed at 14, 30, 60 and 168 days (fermentative system), 11, 35 and 52 days (Fe(III)-reducing system) and 14, 35, 60 and 120 days (SO_4^{2-}-reducing system) and the pH was measured. Cation (B, Si, Ca, Na, P, Zr, Al) concentrations in solution were measured by ICP-OES (Perkins Elmer Optica 5300). Anion (sulphate, phosphate) and volatile fatty acids (VFA's) concentrations in solution were measured by ion chromatography. Glass dissolution rates were calculated from the normalized mass loss of boron over time in g m^{-2} d^{-1} (Eq. 1) where NL_B is the normalised mass loss for boron in g m^{-2}; C_B is the average concentration of boron released from the glass at a particular time point in mg L^{-1}; $C_{B,b}$ is the average concentration of boron in the media only blank, in mg L^{-1}; SA is the surface area of the exposed glass in m^2; and V is the volume of leachant in m^3.

$$NL_i = \frac{(C_i - C_{i,b})V}{f_i SA} \quad (1)$$

For later time-points, the total boron released was corrected to account for boron removed at previous time-points e.g. total mass of boron released from the glass = (C_{T1} x V_{T1}) + (C_{T2} x V_{T2}) + (C_{T3} x V_{T3}) + ($C_{remaining}$ x $V_{remaining}$) where V is the volume of solution removed and C is the concentration of boron in that solution.

2.4. Imaging of microbial cells on glass surfaces

The presence of live and dead microbes and biofilm on the surface of one of the glass monoliths was confirmed by live/dead staining followed by epifluorescence microscopy (microscope, Zeiss Axio imager A2) according to the method described in Buolos et al., (1999) [13]. The other glass monolith was prepared for environmental scanning electron microscopy (ESEM). Cells were preserved by soaking in: (i) glutaraldehyde (2.5%) overnight; (ii) 60 mL of glutaraldehyde (2.5%) and 40 mL phosphate buffered saline (PBS – 8 g NaCl,0.2 g KCl, 1.42 g Na_2HPO_4, 0.27 g KH_2PO_4, 1 L H_2O) for 2 h; (iii) 30 mL glutaraldehyde (2.5%) and 70 mL PBS for 2 h; then (iv) PBS for 2 h. Samples were then soaked in ethanol solutions of increasing concentration (25, 30, 40, 50, 60,70 80%, 90% and 100%) each for 30 min, pipetting off the previous solution before adding the next. Monolith samples were imaged uncoated by ESEM (FEI Quanta 650 FEG-ESEM) under low vacuum and in secondary electron and backscattered electron detection mode.

2.5. 16S rRNA gene sequencing analysis of microbial communities

16 S polymerase chain reaction (PCR) ribosomal ribonucleic acid (rRNA) gene analysis was performed on raw sediment, on each inoculum before it was added to glass-microbe experiments, and on each monolith system after 60 days' incubation. Samples were taken both from the solution and from the surface of the glass by rinsing/scraping. Deoxyribonucleic acid (DNA) was extracted from solid samples directly from swabs using a DNeasy PowerSoil Pro Kit (Qiagen, Manchester, U.K). Sequencing of PCR amplicons of 16 S rRNA genes was conducted with the Illumina MiSeq platform (Illumina, San Diego, CA, USA) targeting the V4 hyper variable region (forward primer, 515 F, 5′-GTGYCAGCMGCCGCGGTAA-3′; reverse primer, 806 R, 5′-GGACTACHVGGGTWTCTAAT-3′) for 2 × 250-bp paired-end sequencing (Illumina) [16,17]. PCR amplification was performed using Roche FastStart High Fidelity PCR System (Roche Diagnostics Ltd, Burgess Hill, UK) in 50 µl reactions under the following conditions: initial denaturation at 95 °C for 2 min, followed by 37 cycles of 95 °C for 30 s, 55 °C for 30 s, 72 °C for 1 min, and a final extension step of 3 min at 72 °C. The PCR products were purified and normalised to ~20 ng each using the SequalPrep Normalization Kit (Fisher Scientific, Loughborough, UK). The PCR amplicons from all samples were pooled in equimolar ratios. The run was performed using a 4.5 pM sample library spiked with 4.5 pM PhiX to a final concentration of 12% following the method of Schloss and Kozich [41].

For QIIME2 analysis, sequences were imported into QIIME2 q2cli v2021.04 [14]. The sequences were trimmed with cutadapt, visually inspected with demux, and denoised with DADA2 [54] to remove PhiX contamination, trim reads, correct errors, merge read pairs and remove PCR chimeras. Representative amplicon sequence variant (ASV) sequences and their abundances were extracted by feature-table [12]. QIIME2 plugins were executed with DADA2 quality settings "- -p-trunc-len-f" of 230 and "- -p-trunc-len-r" of 220. Taxonomical assignment was obtained with the *q2-feature classifier* plugin [67] using the classify-sklearn naïve Bayes taxonomy classifier against the Silva v138 99% reference sequence database [14,71]. Contaminant sequences identified in extraction and PCR controls were manually removed.

2.6. Post dissolution chemical analysis of the glass surface

Post dissolution analysis of the glass surface and mineral precipitates was performed by X-ray diffraction (Bruker D2 Phaser X-ray Diffractometer (Cu Kα radiation) between 5° and 70° 2θ with a step size of 0.02° and sample rotation of 60 Hz) and laser ablation-mass spectrometry (ImageGEO193- Elemental Scientific Lasers with 8900 series ICP-MS/MS- Agilent Technologies) to analyse the chemistry of micron scale alteration layers present on altered glass samples. During laser

ablation, successive pulses (duration 0.2 s; frequency 5 Hz), were used to estimate the chemistry of the glass surface at approximately 0.1 μm depth intervals.

3. Results and discussion

A range of anaerobic microcosm incubations were set up using defined selective media to probe the impact of microbial metabolism on glass dissolution. The results of glass dissolution in the absence of microbes are described first, then the effect of the glass on the microbial community is evaluated, and finally the effect of the microbes on glass dissolution in the different systems are described.

3.1. Abiotic dissolution of phosphorus containing glasses

The dissolution of borosilicate glass is quantified by measuring the accumulation of boron in solution. Boron is chosen because, in most systems, it remains in solution as boric acid (H_3BO_3) or borate ($B(OH)_4^-$) and is not retained in the hydrated silica gel layer. However, the iron phosphate glass does not contain boron or any other species that would not be retained in the alteration layer, so it was not possible to accurately quantify glass dissolution by measuring the accumulation of ions in solution. In abiotic 'glass only' systems, the normalized mass loss of boron revealed the significant influence of media composition, as well as glass composition, on dissolution rates (Fig. 2), highlighting the need for a separate 'glass only' abiotic control for each glass in each system in order to separate biotic effects from abiotic effects.

As the pH remained constant (within 0.5 of the starting pH of 8.5) across all systems (SI Figs. 2, 3 and 4), differences in glass dissolution between systems must result from variables in the solution chemistry (Table 2 and Table 3). In general, glasses dissolved slowest in the FW media amended with glucose, faster in the Postgate C media and fastest in the FW media amended with Fe(III)-citrate (Fig. 2). This trend correlated with increasing aqueous Fe(III) concentrations (3.6×10^{-3} mM, 1.79×10^{-2} mM and 55 mM in the FW medium amended with glucose, Postgate C medium and FW medium amended with Fe(III)-citrate respectively). Fe(III) and Mg (present in SO_4^{2-}-reducing medium at 2.72×10^{-1} mM and FW media at 2.9×10^{-2} mM (Table 2)) have both been shown to increase glass dissolution. They have a high affinity for Si, and readily form silicate minerals at the glass surface that can disrupt gel layer formation and drive glass dissolution (e.g. [3,4,7,25,26]). Citrate has also been shown to enhance silicate mineral weathering by forming a soluble silica-citrate complex and may slow or prevent the formation of a protective silica gel layer on silicate glasses [10]. Although citrate will mostly be bound as Fe(III)-citrate in these systems, its influence must be considered.

More surprisingly, the relative durability of the four borosilicate glasses changed as function of solution chemistry and this was tentatively linked to the presence of Fe(III) in solution. In FW media containing negligible Fe(III), a decrease in the rate of glass dissolution was observed across glasses 1–4 as P_2O_5 content increased from 0 to 1.3 mol %. However, in FW media, containing high Fe(III) in the form of Fe(III)-citrate, the rate of glass dissolution increased with increasing P_2O_5 suggesting an interaction between Fe(III) and P.

Post dissolution analysis of glass powders by XRD did not detect any crystalline phases, indicating that any secondary phases formed were either non-crystalline or crystals were too few or too small to be detected. PHREEQC modelling of the solution chemistry in each abiotic system (Thermochimie database_v11) suggests super-saturation with regard to various mineral phases including clays, aluminium hydroxide and Ca-phosphate (including hydroxyapatite) where phosphorus was present (SI Tables 2–7). Where both iron and phosphate were present, PHREEQC modelling predicted supersaturation with regard to strengite ($Fe(III)PO_4$). Analysis of alteration layer chemistry by laser ablation ICP-MS, conducted on glasses altered in sulphate reducing media, confirmed that P and Mg concentrations were both elevated in the top 0.5 μm of the glass surface indicating their accumulation in the alteration layer (SI Fig. 5).

3.1.1. Abiotic glass alteration in the absence of Fe

Two factors may contribute to the trend of increasing durability with increasing P_2O_5 observed in solutions with low concentrations of Fe(III). Firstly, phosphorus addition may have increased the intrinsic durability of the glass by inducing re-polymerisation of the silicate network as described by Love et al. [50]. The addition of P_2O_5 to borosilicate glasses has been reported to form isolated $P_2O_7^{4-}$ or PO_4^{3-} anions and $P_2O_7^{4-}$ anions that connect preferentially to borate groups. These species require alkali cations for charge compensation that they scavenge from the silicate network leading to a reduction in non-bridging oxygens and, subsequently, a higher degree of polymerisation [24,50,60,73].

Secondly, as indicated by solution data and post dissolution surface analysis, phosphorus was retained in the alteration layer where it may have slowed the rate of dissolution. The borosilicate glasses (glasses 1–3) are similar in composition to 'bioglass', Ca and P containing glasses designed to bond to, and stimulate new bone growth by forming an amorphous film of Ca-P that alters over time to stoichiometric (Ca/P ratio 1.67) or non-stoichiometric hydroxyapatite (typical bioglass

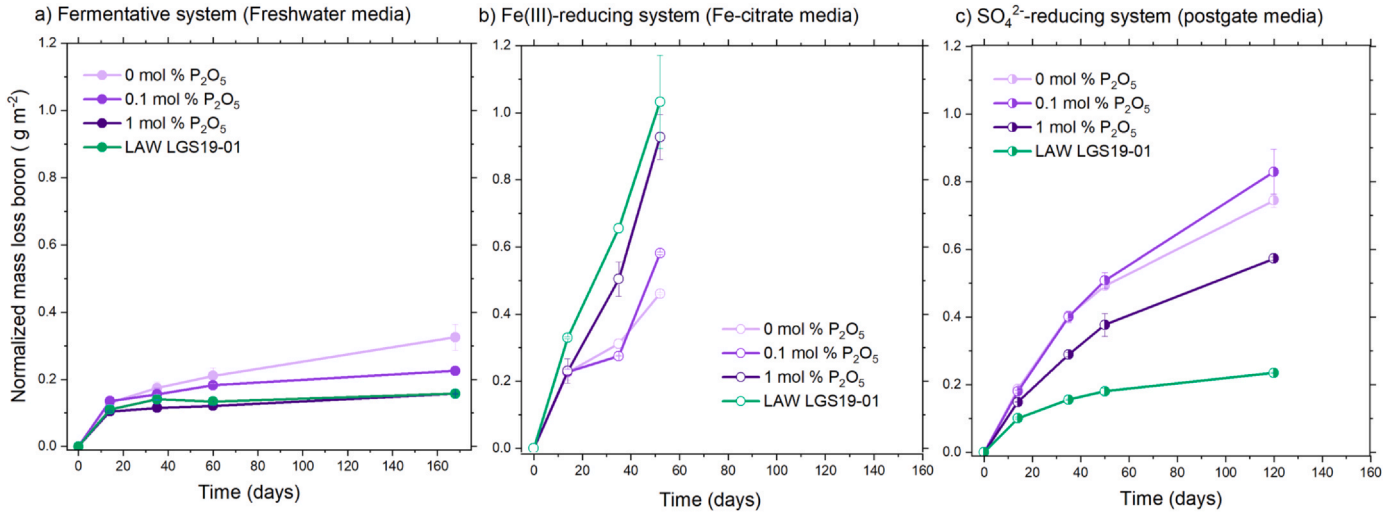

Fig. 2. Abiotic dissolution behaviour of glasses 1–4 in the three different growth media; a) fermentative system (FW media), b) Fe(III)-reducing system (FW media amended with Fe(III)-citrate) and c) SO_4^{2-}-reducing system (Postgate-C media).

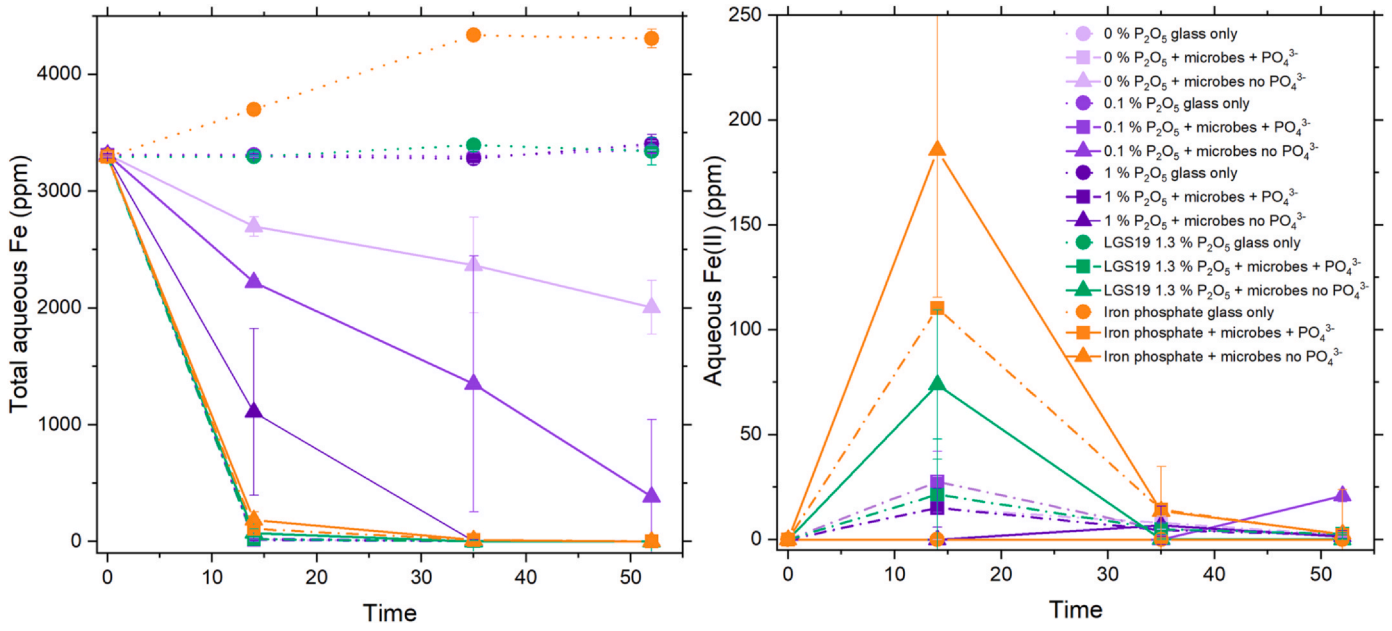

Fig. 3. Left: total aqueous Fe as measured by ICP-OES for the five glasses. Right: aqueous Fe(II) as measured by Ferrozine assay for the five glasses. Dotted lines = glass only systems, dash-dot lines = systems amended with microbes and PO_4^{3-} and solid lines = systems amended with microbes and no PO_4^{3-}. Errors represent the standard deviation of duplicate measurements (glass only systems) and triplicate measurements (microbially amended systems).

compositions: 45–64 mol% SiO_2; 5–6 mol% P_2O_5; 25–30 mol% CaO and 20–30 mol% Na_2O) [72,78]. In studying the effect of similar concentrations of PO_4^{3-} on glass dissolution at 90 °C, Gin et al. attributes an increase in glass dissolution to the formation of microcrystalline phosphate phases, including Ca and rare earth-phosphates as evidenced by TEM, in the gel layer, altering its microstructure and rendering it less protective [29]. In this study conducted at 30 °C, although phosphorus concentrations were elevated at the glass surface (top 0.5 μm) relative to the bulk glass, calcium was depleted (SI Fig. 5). In these low temperature systems, it must be concluded either that crystalline Ca-phosphate phases did not form, or their formation was not detrimental to the protective qualities of the gel layer.

3.1.2. *Abiotic glass alteration in the presence of Fe*

Glass dissolution rates were generally higher in the Fe(III)-reducing systems (50 mM Fe(III)-citrate), and glass dissolution increased with increasing P_2O_5 (Fig. 7). It is known that Fe(III) can combine with Si in the glass alteration layer to form iron silicates that disrupt the formation of a passivating gel layer and decrease silica saturation to promote further dissolution of the gel layer (e.g. [3]). However, this study suggests that the combination of Fe(III) and P may also negatively impact glass durability. It is possible that Fe phosphate phases can have a similar effect to that of rare earth and Ca phosphates observed in studies by Gin et al., [29]. In Gin et al.'s study there was also Fe, along with some Mn and Zn, sourced from the SON68 glass found to be associated with the Ca and P [29]. In aqueous environments, the rapid reaction of Fe(III) with orthophosphate (PO_4^{3-}) to form Fe(III)-phosphate phases, e.g., strengite ($FePO_4.2\,H_2O$), results in the formation of small, stable amorphous colloids. As Fe(III) has a high affinity for silica, and is known to sequester to the gel layer, it is therefore possible that aqueous Fe(III) could react with P within the protective gel layer in these systems causing detrimental changes to its microstructure (e.g. [52,91]).

3.2. *Effect of phosphorus containing glass on microbial growth, respiration and diversity*

A range of anaerobic microcosms incubations were set up using defined selective media to probe the impact of microbial metabolism on glass dissolution. Overall, across the three systems, utilization of available electron donors by the microbial consortium was fastest in systems where phosphate (PO_4^{3-}) was included in the systems, slower in systems where the only source of phosphorus was the glass (glasses 2–5), and slowest when the glass contained no phosphorus (glass 1).

3.2.1. *Effect of glass composition on microbial growth and respiration*

In fermentative systems, accumulation of fermentation products (VFAs: acetate, lactate, propionate, isobutyrate) were monitored in solution. In all systems where PO_4^{3-} was present in growth media, fermentation was uninhibited and breakdown of glucose to VFAs and then subsequent utilisation of VFAs was complete within two weeks (i.e. before the first sampling point) (Table 5). Similarly, in systems containing glass 5 (iron phosphate glass; 53 mol% P_2O_5) with no added PO_4^{3-}, aqueous PO_4^{3-} at two weeks measured 102.4 ± 5.8 mg L^{-1}, meaning that P release from glass 5 was sufficiently high that fermentation was uninhibited and all VFAs were consumed within two weeks (Table 5). In systems containing borosilicate glass where the only source of phosphorus was the glass, PO_4^{3-} concentrations remained below the limit of detection and fermentation proceeded at a slower rate. Glucose was broken down more slowly and, after two weeks, VFA concentrations were correlated with increasing P_2O_5 content in the glass: VFAs in glass 4 (1.3 mol% P_2O_5) > glass 3 (1 mol% P_2O_5) > glass 2 (0.1 mol% P_2O_5) ~ glass 1 (0 mol% P_2O_5) (Table 5). The fact that some microbial activity was still detected in systems with no phosphorus in either the glass or media was likely due to carry over of phosphorus from the biomass inocula. Live/dead staining followed by epifluorescence microscopy confirmed the presence of living cells in all fermentative systems (SI Fig. 6).

In the Fe(III)-reducing system, microbial activity was tracked by measuring total aqueous Fe and Fe(II) in solution (Fig. 3), and by observing the precipitation of Fe(II)-biominerals and a change in solution colour from orange to colourless (SI Fig. 7). Total Fe concentrations remained constant for all control systems, except glass 5 (iron phosphate) where total Fe increases as iron was released from the glass (Fig. 3). Meanwhile, a decrease in aqueous Fe was observed in all microbially active systems consistent with the breakdown of Fe(III)-citrate, reduction to Fe(II) (confirmed by ferrozine assay) (Fig. 3) and subsequent formation of Fe(II)-bearing biominerals (SI Fig. 8). Mineral phases formed were confirmed by XRD to be primarily siderite, with

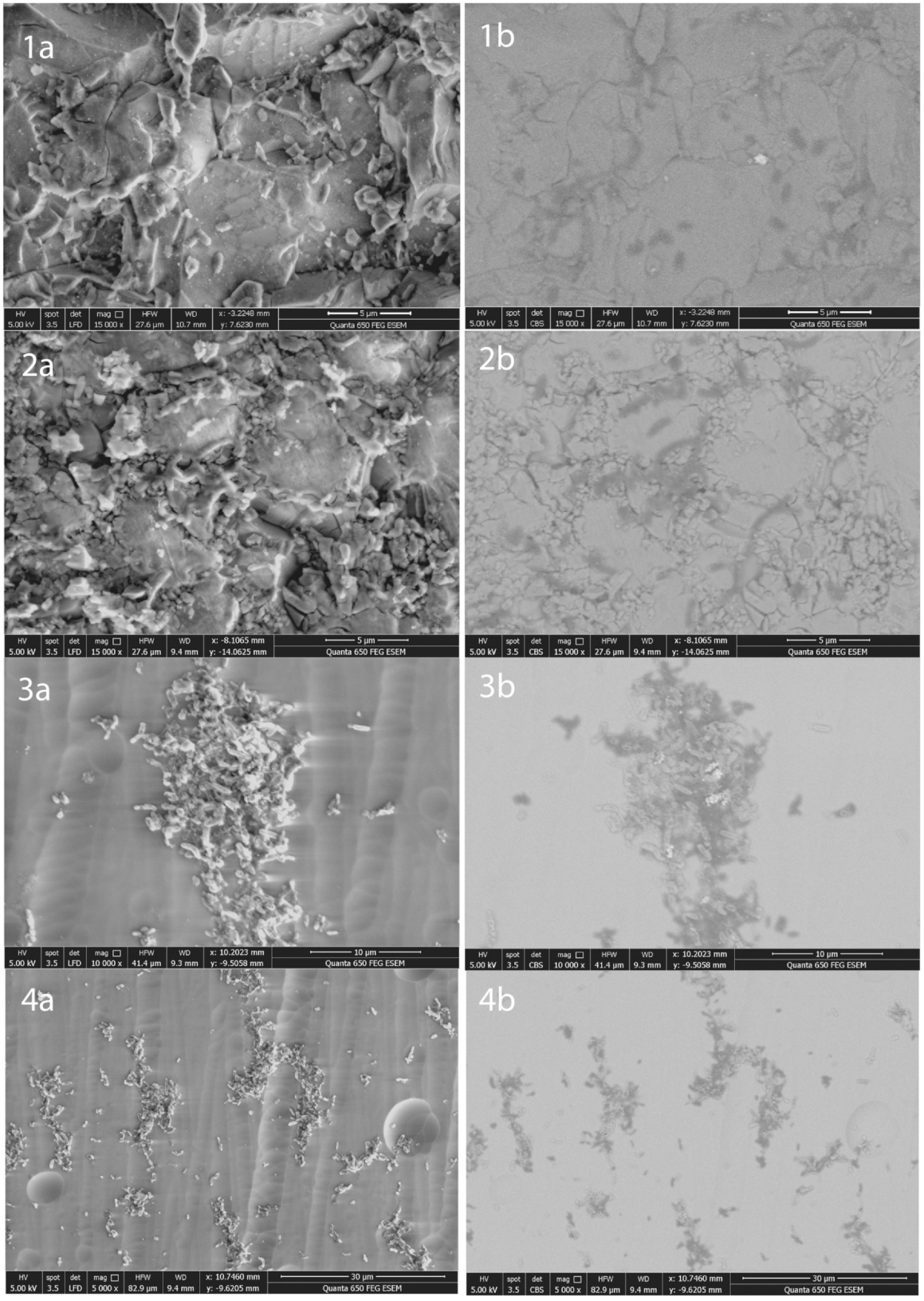

Fig. 4. ESEM images of microbial cells on 1) LAW glass in a) SE mode and b) BSE mode, 2) borosilicate glass with 1% P_2O_5 in a) SE mode and b) BSE mode, 3 & 4) iron phosphate glass in a) SE mode and b) BSE mode. 1 and 2 show small groups of cells whereas 3 and 4 show biofilm formation.

vivianite also forming where PO_4^{3-} was present in solution (SI Fig. 8; [87]). Reduction of Fe(III)-citrate was complete by the first timepoint (14 days) in systems with added PO_4^{3-} (Fig. 3). As in fermentative systems, where the only source of phosphorus was the glass, reduction proceeded in the order glass 5 (53 mol% P_2O_5) > glass 4 (1.3 mol% P_2O_5) > glass 3 (1 mol% P_2O_5) > glass 2 (0.1 mol% P_2O_5) > glass 1 (0 mol% P_2O_5). Live/dead staining followed by epifluorescence microscopy revealed live cells on the surface of all glass monoliths (SI Fig. 6),

Table 5
Concentration of the selected anions phosphate (PO_4^{3-}), acetate (CH_3COO^-), propionate ($CH_3CH_2COO^-$), Isobutyrate ($(CH_3)_2CHCOO^-$) and Isovalerate ($(CH_3)_2CHCH_2COO^-$) after 14 days.

Glass	Media	Phosphate mg L^{-1}	Acetate mg L^{-1}	Propionate mg L^{-1}	Isobutyrate mg L^{-1}	Isovalerate mg L^{-1}
Glass 1	+ PO_4^{3-}	460.6 ± 31.4	Below LOD	Below LOD	Below LOD	Below LOD
0 mol% P_2O_5	No PO_4^{3-}	Below LOD	166.1 ± 2.3	5.1 ± 0.3	0.4 ± 0.2	0.3 ± 0.02
Glass 2	+ PO_4^{3-}	440.6 ± 54.9	Below LOD	0.6 ± 0.1	Below LOD	Below LOD
0.1 mol% P_2O_5	No PO_4^{3-}	Below LOD	165.1 ± 49.8	0.7 ± 0.4	0.2 ± 0.1	0.3 ± 0.1
Glass 3	+ PO_4^{3-}	469.8 ± 12.8	Below LOD	Below LOD	Below LOD	Below LOD
1 mol% P_2O_5	No PO_4^{3-}	Below LOD	208.8 ± 70.26	14.8 ± 19.83	0.5 ± 0.4	0.3 ± 0.03
Glass 4	+ PO_4^{3-}	669.6 ± 0	2.3 ± 0	0.3 ± 0	Below LOD	Below LOD
LAW LGS19–01	No PO_4^{3-}	Below LOD	397.3 ± 41.0	73.3 ± 0	1.0 ± 0.3	0.8 ± 0.2
Glass 5	+ PO_4^{3-}	655.8 ± 19.4	Below LOD	Below LOD	Below LOD	Below LOD
Iron phosphate	No PO_4^{3-}	102.4 ± 5.8	Below LOD	Below LOD	Below LOD	Below LOD

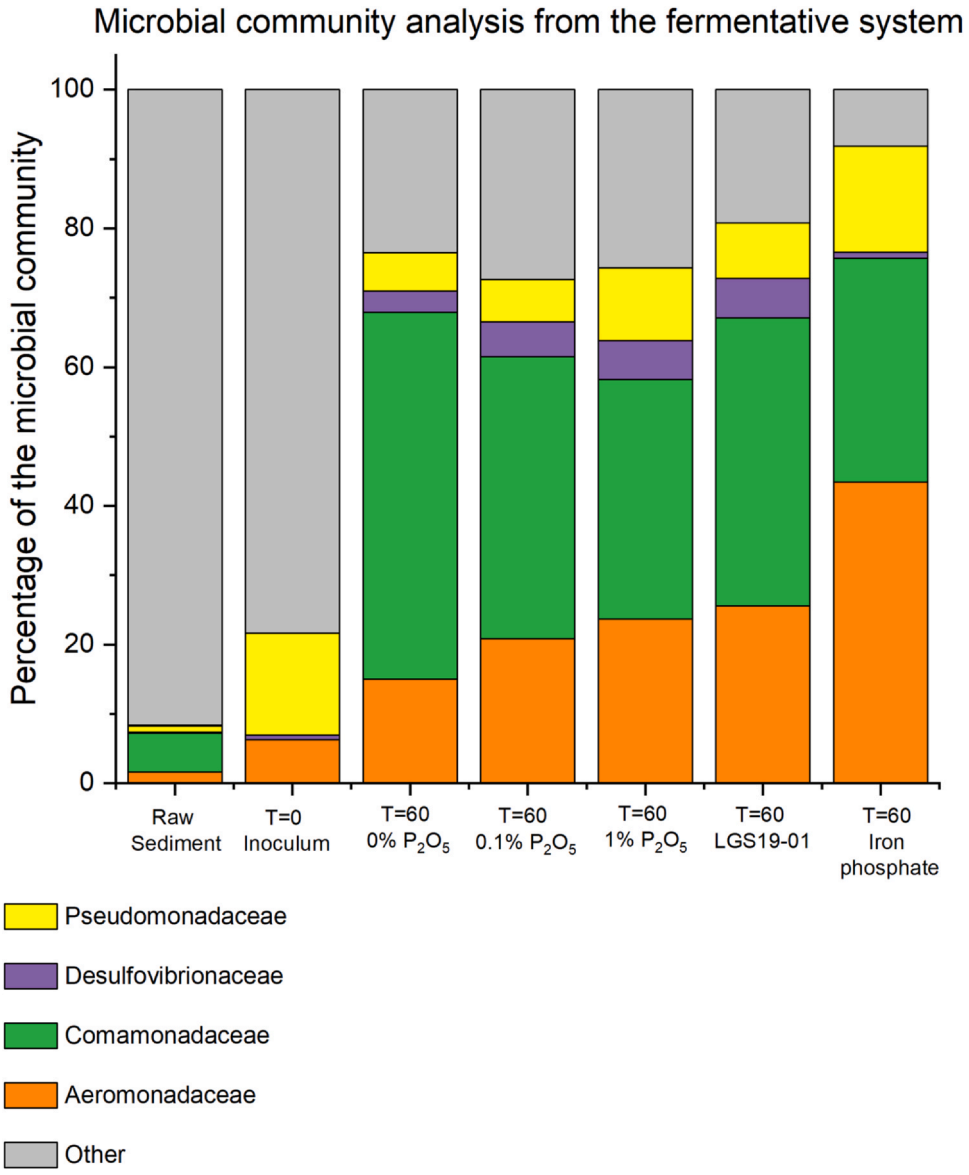

Fig. 5. Microbial community analysis from the anaerobic system showing breakdown of the community at the family level. Samples taken from glass monoliths in experiments in media without added PO_4^{3-} after time (T) = 60 days.

however, the lack of Fe(II) in solution indicates that metabolic activity was limited when the glass did not contain P_2O_5.

In SO_4^{2-}-reducing systems, utilization of lactate and acetate was faster in experiments amended with PO_4^{3-} than in those where the only source of phosphorus was the glass (SI Table 8), however, no clear trend in electron donor utilization was observed between the different glasses, likely due to the wide spacing of time points. For this system, cells on the surface of the monoliths from the SO_4^{2-}-reducing system were imaged using ESEM. Cells displayed typical 'bacillus' morphology in secondary electron (SE) mode and as 'dark' low z-contrast areas in

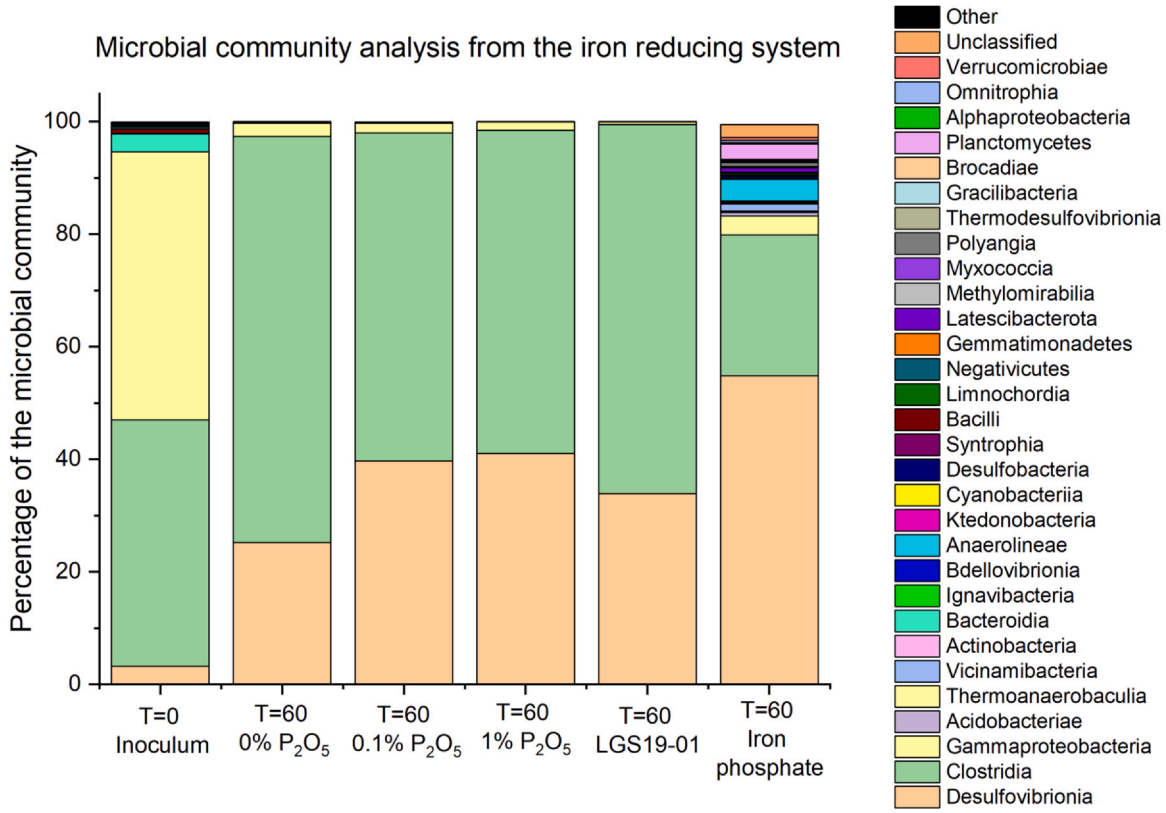

Fig. 6. Microbial community analysis from the Fe(III)-reducing system. Samples taken from glass monoliths in experiments in media with no added PO_4^{3-} after 60 days.

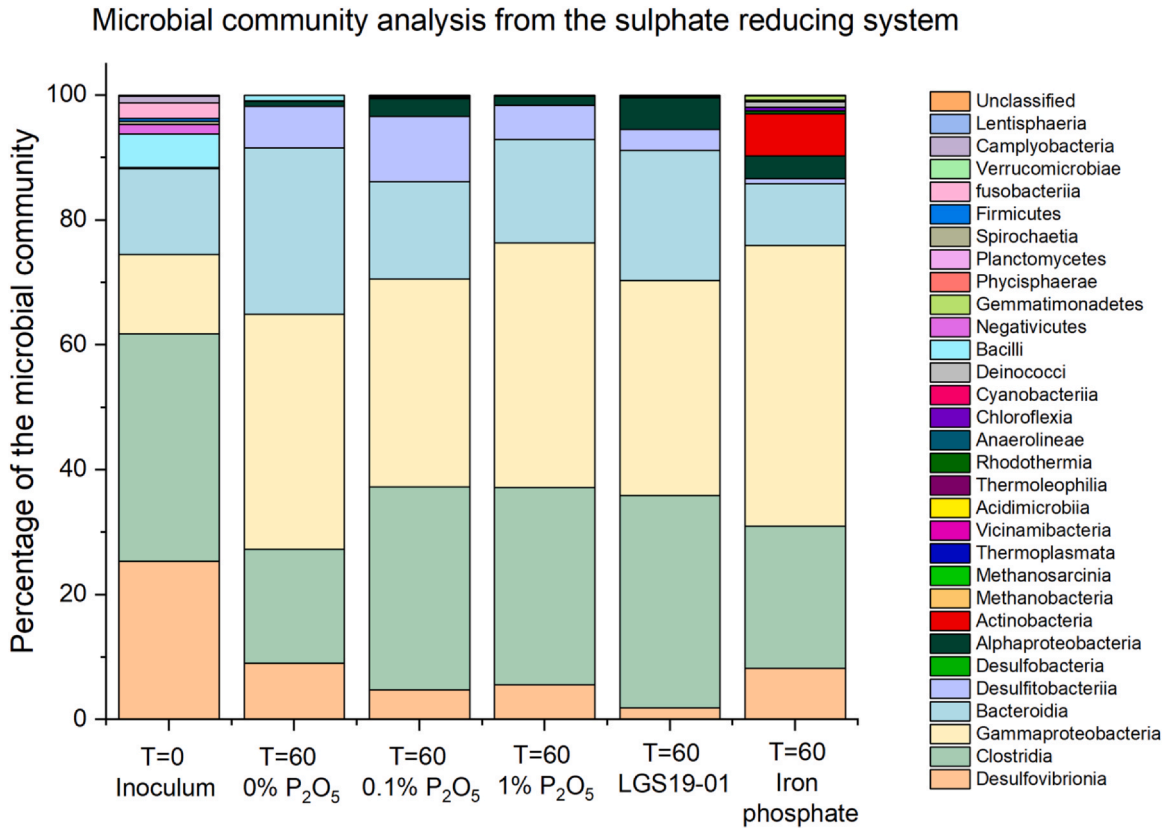

Fig. 7. Microbial community analysis from the SO_4^{2-}-reducing system. Samples taken from glass monoliths in experiments in media with no added PO_4^{3-} after 60 days.

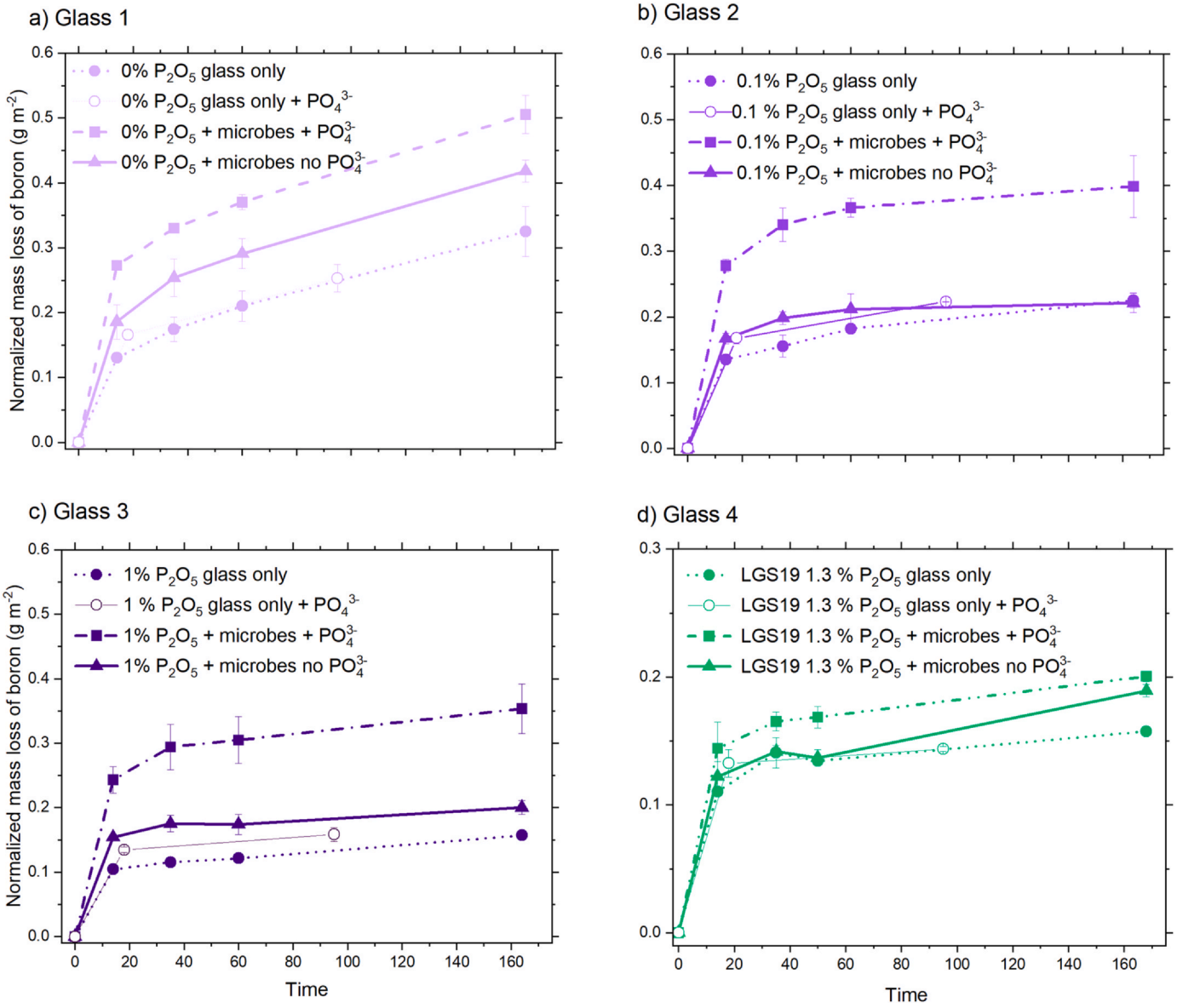

Fig. 8. Normalized mass loss of boron for borosilicate glasses 1–4 in the fermentative system where glucose was added as the electron donor. Error bars are the standard deviation of triplicate measurements. Note the different normalised mass loss scale for glass 4 (LAW LGS19).

backscattered electron (BSE) mode. Only isolated cells were observed on glasses 1 and 2, containing no P_2O_5 and 0.1 mol% P_2O_5 respectively, small cell groups were associated with the surface of glasses 3 and 4, containing 1 and 1.3 mol% P_2O_5 respectively, and a dense microbial colony was observed on the surface of glass 5 (Fig. 4). Glass 5 (the iron phosphate glass) contained ~ 30.4 mol% Fe_2O_3, of which Fe(II) comprised the minority (typical Fe(II)/Fe_{total} ratios are 0–0.2) [35,39]. It is possible that Fe(III) could be used as an electron acceptor in anaerobic respiration as has been postulated for iron-containing basaltic glasses, and this could account for the greatly increased colonisation of the iron phosphate glass surface [63,81].

3.2.2. *Effect of glass composition on microbial community composition and diversity*

Distinct microbial communities evolved when the microbial inoculum from Harpur Hill, Buxton, was subcultured in different media to support fermentation, Fe(III) reduction, or SO_4^{2-} reduction (Table 4; SI Fig. 9; SI Table 9). At the class level, the starting inoculum for the fermentative systems after six successive subcultures in glucose-amended medium was dominated by *Gammaproteobacteria*, *Negativicutes, Clostridia* and *Bacteroidia.* The starting inoculum for the Fe (III)-reducing systems was dominated by *Gammaproteobacteria*, *Clostridia* and *Desulfovibrionia*, and known Fe(III)-reducing species present from the genera *Aeromonas (*4.63%*)* (e.g. [42]) and *Shewanella (*8.29%*)* (SI Fig. 9; SI Table 9). The starting inoculum for the SO_4^{2-}-reducing systems was dominated by *Gammaproteobacteria*, *Clostridia* and *Desulfovibrionia*, and enriched in the known SO_4^{2-}-reducing species most closely related to *Desulfovibrio desulfuricans* (26.6%) (SI Fig. 9: SI Table 9).

The 16S rRNA gene sequencing of the initial inoculum was compared with that for samples taken from monolith systems after 60 days incubation to assess changes in the microbial community. Samples were taken from the solution and sterile swabs were scraped across the surface of the glass in an attempt to obtain only those cells most closely associated with the glass. For the four borosilicate glasses (glasses 1–4) there was no obvious difference in the composition of the microbial community at the class level regardless of phosphorus content (Figs. 5–7; SI Tables 10–12; SI Fig. 10–12). Similarly, there was no obvious difference between the microbial community associated with the glass surface and the microbial community sampled from the

Table 6
Dissolution rates based on the normalised mass loss of boron for glasses 1–4 at 30 °C in the fermentative system.

Glass	Conditions	Time frame	Rate (g m^{-2} d^{-1})
Glass 1–0% P_2O_5	Glass only	0–14 days	4.59 (± 0.53) x 10^{-3}
		35–164 days	1.14 (± 0.27) x 10^{-3}
	Glass + microbes + PO_4^{3-}	0–14 days	9.43 (± 0.08) x 10^{-3}
		35–164 days	1.24 (± 0.26) x 10^{-3}
	Glass + microbes no PO_4^{3-}	0–14 days	7.46 (± 0.95) x 10^{-3}
		35–164 days	1.13 (± 0.11) x 10^{-3}
Glass 2–0.1% P_2O_5	Glass only	0–14 days	4.44 (± 0.48) x 10^{-3}
		35–164 days	5.24 (± 0.07) x 10^{-4}
	Glass + microbes + PO_4^{3-}	0–14 days	9.73 (± 0.72) x 10^{-3}
		35–164 days	4.36 (± 0.24) x 10^{-4}
	Glass + microbes no PO_4^{3-}	0–14 days	5.84 (± 0.24) x 10^{-3}
		35–164 days	1.72 (± 0.06) x 10^{-4}
Glass 3–1% P_2O_5	Glass only	0–14 days	3.29 (± 0.07) x 10^{-3}
		35–164 days	3.15 (± 0.01) x 10^{-4}
	Glass + microbes + PO_4^{3-}	0–14 days	8.40 (± 0.10) x 10^{-3}
		35–164 days	2.67 (± 0.49) x 10^{-4}
	Glass + microbes no PO_4^{3-}	0–14 days	5.24 (± 0.17) x 10^{-3}
		35–164 days	1.87 (± 0.46) x 10^{-4}
Glass 4 - LGS19–01	Glass only	0–14 days	4.02 (± 0.03) x 10^{-3}
		35–164 days	1.25 (± 0.70) x 10^{-4}
	Glass + microbes + PO_4^{3-}	0–14 days	4.71 (± 0.20) x 10^{-3}
		35–164 days	2.66 (± 0.37) x 10^{-4}
	Glass + microbes no PO_4^{3-}	0–14 days	4.04 (± 0.14) x 10^{-3}
		35–164 days	3.58 (± 0.23) x 10^{-4}

solution for the four borosilicate glass systems, beyond variation in the evenness (proportion of each class) (SI Fig. 11 and 12; SI Tables 11 and 12).

In contrast, a more diverse community was associated with the dense microbial biofilm on the surface of the iron phosphate glass (glass 5). In the fermentative system, 16 S rRNA gene analysis showed a notable increase in the relative abundance of *Aeromonas* species, from 22% to 25% on the borosilicate glasses systems to 43% on surface of iron phosphate glasses (Fig. 5). *Aeromonas* species are capable of Fe(III) reduction in a variety of environments (e.g. [27,92]).

In the Fe(III)-reducing system (Fig. 6), 16 S rRNA gene sequencing revealed a more diverse community associated with the surface of the iron phosphate glass than the four borosilicate glasses. Shannon indices were 0.69, 0.76, 0.74, 0.67 and 1.50 respectively for glasses 1–5) and there was a notable increase in species most closely related to *Desulfovibrio desulfuricans* (capable of Fe(III)-reduction).

In the SO_4^{2-}- reducing system, the Shannon diversity index of the community associated with glass 5 was 1.62 in comparison to 1.51, 1.54, 1.42 and 1.43 for glasses 1–4 respectively. This indicates a slightly more diverse community associated with the biofilm on the surface of the iron phosphate glass (Fig. 4) compared to the microbial community associated with the sporadic cell coverage on the borosilicate glasses (glasses 1–4, Fig. 4).

3.3. Microbial effects on the dissolution of phosphorus containing glasses

In this study, microbes influenced glass dissolution rates in almost all systems tested, in some causing an increase in dissolution rate and in other cases a decrease in dissolution rate compared to the corresponding abiotic control. To explain these results, we must consider the different mechanisms by which microbes can influence not only glass dissolution but also the behaviour of the boron tracer.

3.3.1. Microbial effect on the dissolution of borosilicate glasses

With regard to microbial influence on the boron tracer, the potential for sorption or uptake of boron by microbial cells or bio-mineral precipitates must be considered. Boron uptake by microbial cells is likely low, as it is an essential micronutrient required in only small quantities [88]. Here, the highest microbial activity (indicated by electron donor utilization, observation of live cells by epifluorescence and SEM) was often correlated with the highest boron release rates, which confirms that the μM levels of boron were non-toxic, and that boron uptake by cells was negligible. Boron sorption to secondary Fe(II) bearing minerals (siderite and vivianite formed in the Fe(III)-reducing system) was also negligible, as boron concentrations increased continually, and linearly, during their formation. Boron sorption to iron oxide (FeOOH) phases, however, is well documented (e.g. [22]) and, therefore, careful attention was paid to ensure that oxygen ingress into reduced systems did not result in Fe-oxide precipitation.

Microbes can directly influence the glass via contact and secretion of chemicals that increase glass dissolution, or can indirectly influence the glass through changes to the local environment (e.g. pH, solution chemistry, and redox potential). Microbial cells can accelerate the precipitation of mineral/biomineral phases (e.g. [28]). This can occur passively, through providing a nucleation site for minerals that are thermodynamically favourable but kinetically slow to form. Biominerals can also precipitate directly as a result of microbial metabolism, e.g., bio-reduction of Fe(III) to Fe(II) results in the precipitation of biogenic Fe(II) phases in the vicinity of the cell. pH has a major effect on the dissolution rate of borosilicate glass [82] and microbes can change the pH directly, through production of organic acids, or indirectly through consumption/production of H^+/OH^- in metabolic reactions. Here, all systems tested were buffered to pH 8.5 by the buffering capacity of the bicarbonate-based FW and Postgate media (SI Figs. 2, 3 and 4). However, localised pH gradients could form under and around microbial cells/biofilm, at the surface of the glass or between tightly packed glass particles.

In the fermentative system, microbial activity resulted in an increase in glass dissolution during active fermentation. For glasses 1–3, initial boron release rates (< 14 days) were higher in all experiments inoculated with microorganisms when compared to their equivalent abiotic control (Fig. 8), and highest in systems with added PO_4^{3-}, where

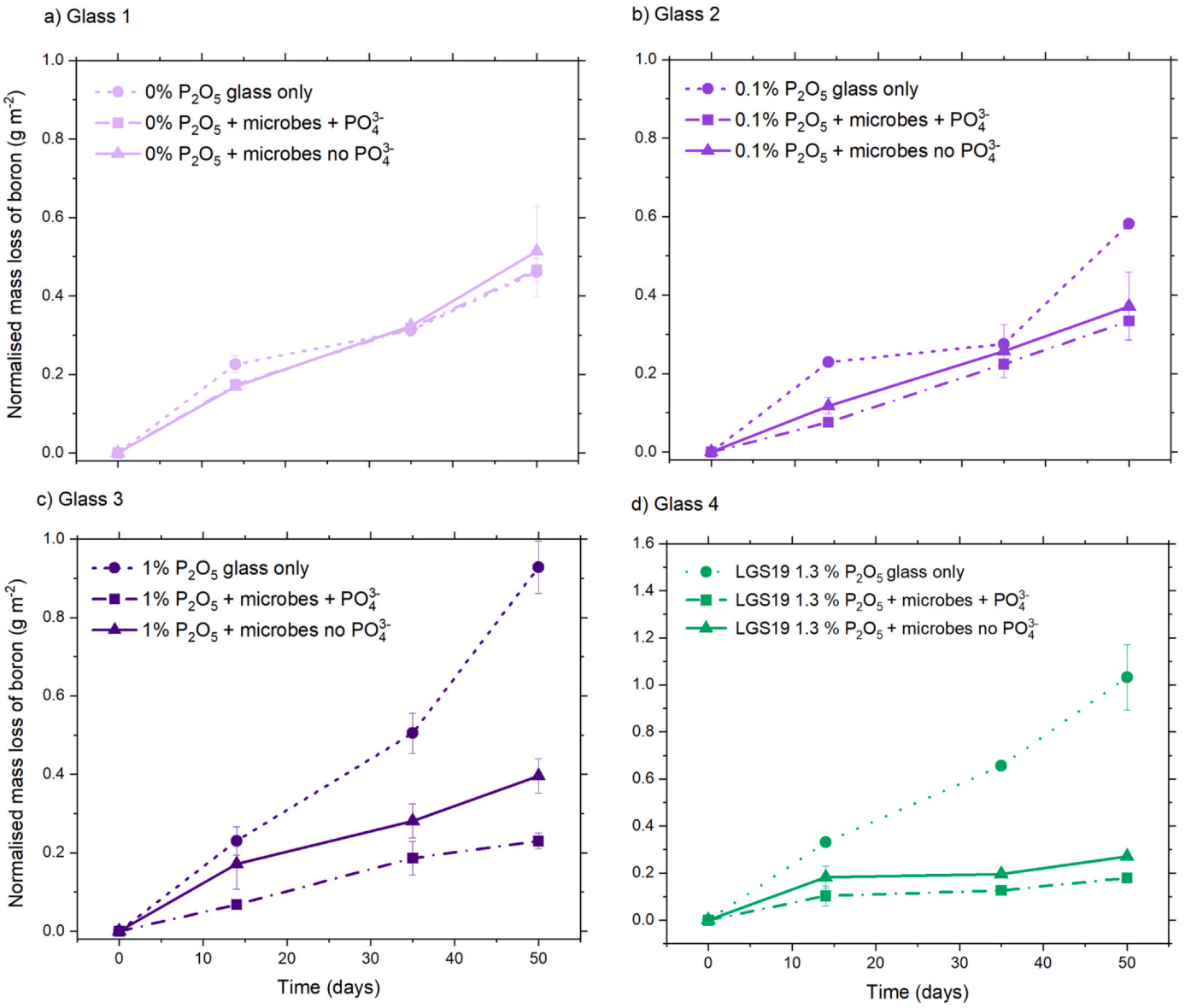

Fig. 9. Normalized mass loss of boron for borosilicate glasses 1–4 in the iron-reducing system where lactate and acetate was added as the electron donor. Error bars are the standard deviation of triplicate measurements. Note the different normalised mass loss scale for glass 4 LAW LGS19.

microbial activity was not limited by phosphorus availability (Table 5). For glass 4 the same trends were observed at 14 days but the increase in boron released was so slight as to be within analytical error (Fig. 8d). Separate control systems with added PO_4^{3-} confirmed that PO_4^{3-} addition alone had a minor effect (as expected under alkaline conditions where anion sorption is limited) (Fig. 8). It is likely that the metabolism of glucose to produce of VFAs, and subsequent change in solution chemistry (and potentially localised pH in the vicinity of cells) was responsible for increased glass corrosion in these initial days. Once VFAs were depleted (> 14 days), boron release rates continued at a similar or lower rate than in the corresponding abiotic control (Fig. 8; Table 6).

Studies into the weathering of natural glasses and rock forming minerals have demonstrated that the release of VFAs/organic acids by microbial cells/biofilm can enhance weathering of mineral surfaces primarily by lowering the pH in the locality of cell (e.g. [11]; Rogers et al., 2004). Although significant pH change in the bulk solution was not observed (SI Fig. 2), localised pH changes around microbial cells and between aggregated glass particles were possible in these systems. Due to the finite availability of an electron donor (glucose) in these systems, the enhanced glass dissolution was short lived and dissolution rates from 14 days onwards were slower for all four borosilicate glasses. Rates from 35 to 164 days decreased with increasing concentrations of P in glass (e.g for systems with added PO_4^{3-} rates were $1.24 \pm 0.26 \times 10^{-3}$ (glass 1) > $4.36 \pm 0.24 \times 10^{-4}$ (glass 2) > $2.67 \pm 0.49 \times 10^{-4}$ (glass 3) = $2.66 \pm 0.37 \times 10^{-4}$ (glass 4) g m^{-2} d^{-1} (Table 6). Previous studies have shown that a microbial biofilm can protect the glass surface and limit the release of elements into solution (e.g. [5,6]). Biofilm formation was not investigated for powdered glass systems, however, in monolith systems extensive surface colonisation

Table 7
Dissolution rates based on the normalised mass loss of boron for glasses 1–4 at 30 °C in the iron reducing system in Fe(III)-citrate media.

Glass	Conditions	Time frame	Rate (g m^{-2} d^{-1})
Glass 1–0% P_2O_5	Glass only	0–50 days	9.22 (± 0.05) x 10^{-3}
	Glass + microbes + PO_4^{3-}	0–50 days	9.33 (± 0.58) x 10^{-3}
	Glass + microbes no PO_4^{3-}	0–50 days	1.02 (± 0.23) x 10^{-2}
Glass 2–0.1% P_2O_5	Glass only	0–50 days	1.16 (± 0.07) x 10^{-2}
	Glass + microbes + PO_4^{3-}	0–50 days	6.68 (± 0.9) x 10^{-3}
	Glass + microbes no PO_4^{3-}	0–50 days	7.43 (± 1.75) x 10^{-3}
Glass 3–1% P_2O_5	Glass only	0–50 days	1.85 (± 0.13) x 10^{-2}
	Glass + microbes + PO_4^{3-}	0–50 days	4.60 (± 0.40) x 10^{-3}
	Glass + microbes no PO_4^{3-}	0–50 days	7.91 (± 0.87) x 10^{-3}
Glass 4 - LGS19–01	Glass only	0–50 days	2.0 (± 0.27) x 10^{-2}
	Glass + microbes + PO_4^{3-}	0–50 days	3.58 (± 0.38) x 10^{-3}
	Glass + microbes no PO_4^{3-}	0–50 days	5.40 (± 0.19) x 10^{-3}

was only observed on iron phosphate glass samples. Assuming a similar behaviour in powdered glass systems, surface passivation by biofilm formation is unlikely to have affected glass dissolution in glasses 1–4.

Dissolution rates in the Fe(III)-reducing systems showed a linear trend (Fig. 9) and, in contrast to the fermentative system, dissolution rates in biotic systems were lower than in their corresponding abiotic control (with the exception of glass 1 where no change was observed). In the abiotic control systems, increasing P_2O_5 in glasses 1–4 increased dissolution rates, however, in biotic systems the opposite trend was observed with increasing P_2O_5 content in glasses leading to a decrease in boron release rates in equivalent systems (Fig. 9; Table 7). For systems amended with microbes and PO_4^{3-} dissolution rates (g m^{-2} d^{-1}) decreased in the order: 9.33 (± 0.58) x 10^{-3} (glass 1) > 6.68 (± 0.9) x 10^{-3} (glass 2) > 4.60 (± 0.40) x 10^{-3} (glass 3) > 3.58 (± 0.38) x 10^{-3} (glass 4). For systems amended with microbes but no PO_4^{3-} dissolution rates in g m^{-2} day^{-1} followed the same trend: 1.02 (± 0.23) x 10^{-2} (glass 1) > 7.43 ± 1.75 × 10^{-3} (glass 2) = 7.91 ± 0.87 × 10^{-3} (glass 3) and 5.40 ± 0.19 × 10^{-3} (glass 4). This reverse trend is most likely attributed to the reduction of Fe(III) to Fe(II) by bacteria causing a chemically different environment at the glass-solution interface. The reduction of Fe(III)-citrate in bicarbonate buffered medium resulted in the precipitation of siderite ($Fe(II)CO_3$) and vivianite ($Fe_3(PO_4)_2.8\,H_2O$) (SI Fig. 8), but these minerals did not form a barrier to dissolution. No decrease in dissolution rate was observed in biotic systems containing glass 1 (0 mol% P_2O_5) when PO_4^{3-} was present in solution and biominerals formed, indicating that surface passivation did not take place. In glass 1, where no phosphorus was present in the glass, it is likely that reactions took place outside the glass alteration layer, as negatively charged PO_4^{3-} does not easily sorb to altered glass surfaces under alkaline conditions [29]. In contrast, where phosphorus was a constituent of the glass, reactions may take place within the alteration layer. Although it is not possible for these experiments to determine the exact mechanism, it can be supposed that interactions between Fe(III) and phosphorus negatively affect the protective qualities of the glass alteration layer whilst Fe(II) and phosphorus result in a more protective layer.

In the SO_4^{2-}-reducing system, two competing processes were occurring. Biotic experiments showed a faster dissolution rate over the initial time points (days < 35) (Table 8 and Fig. 10), similar to the fermentative system. This early increase in dissolution is attributed to the production of acetic acid during microbial oxidation of lactate. However, over the longer-term, in systems where phosphorus was present in the glass, biotic systems released less boron into solution than abiotic controls (Table 8 and Fig. 9). Based on the findings from the Fe(III)-reducing systems, it is possible that small quantities of Fe(III) (1.79 ×10^{-2} mM) along with Mg (2.72 ×10^{-1} mM) in the abiotic controls caused a greater increase in glass dissolution rate than microbial Fe(III)-reduction in the biotic systems. Laser ablation ICP-MS estimates the depth of alteration on sulphate reducing samples as 0.5 µm and confirms accumulation of Mg and phosphorus at the sample surface (Fe was not measured but has also been shown to sequester into the silica gel layer from solution; [3]) (SI Fig. 5).

Table 8
Dissolution rates based on the normalised mass loss of boron of glasses 1–4 at 30 °C in SO_4^{2-} reducing system in Postgate C media.

Glass	Conditions	Time frame	Rate (g m^{-2} d^{-1})
Glass 1–0% P_2O_5	Glass only	0–35 days	1.15 (± 0.02) x 10^{-2}
		35–120 days	4.01 (± 0.45) x 10^{-3}
	Glass + microbes + PO_4^{3-}	0–35 days	1.50 (± 0.11) x 10^{-2}
		35–120 days	3.51 (± 0.17) x 10^{-3}
	Glass + microbes no PO_4^{3-}	0–35 days	1.64 (± 0.07) x 10^{-2}
		35–120 days	2.85 (± 0.46) x 10^{-3}
Glass 2–0.1% P_2O_5	Glass only	0–35 days	1.14 (± 0.04) x 10^{-2}
		35–120 days	5.05 (± 0.90) x 10^{-3}
	Glass + microbes + PO_4^{3-}	0–35 days	1.32 (± 0.15) x 10^{-2}
		35–120 days	2.9 (± 0.47) x 10^{-3}
	Glass + microbes no PO_4^{3-}	0–35 days	1.28 (± 0.01) x 10^{-2}
		35–120 days	2.97 (± 0.35) x 10^{-3}
Glass 3–1% P_2O_5	Glass only	0–35 days	0.83 (± 0.19) x 10^{-3}
		35–120 days	3.34 (± 0.15) x 10^{-3}
	Glass + microbes + PO_4^{3-}	0–35 days	1.03 (± 0.18) x 10^{-2}
		35–120 days	1.14 (± 0.17) x 10^{-3}
	Glass + microbes no PO_4^{3-}	0–35 days	1.08 (± 0.08) x 10^{-2}
		35–120 days	1.23 (± 0.43) x 10^{-3}
Glass 4 - LGS19–01	Glass only	0–35 days	4.44 (± 0.05) x 10^{-3}
		35–120 days	9.32 (± 0.46) x 10^{-4}
	Glass + microbes + PO_4^{3-}	0–35 days	4.65 (± 0.33) x 10^{-3}
		35–120 days	5.11 (± 1.04) x 10^{-4}
	Glass + microbes no PO_4^{3-}	0–35 days	5.92 (± 0.78) x 10^{-3}
		35–120 days	1.93 (± 0.72) x 10^{-4}

3.3.2. Dissolution of iron phosphate glasses

Iron phosphate glasses do not contain silicon and therefore do not produce the characteristic silica gel layer formed during dissolution of silicate/borosilicate glasses. Instead, precipitates of ferrihydrite and Fe (III)-phosphate phases are formed under oxic conditions and Fe(II)-phosphates, Fe(II)-sulphides or Fe(II)-carbonates are formed under reducing conditions, depending on the solution chemistry [33,68]. In the present experiments, a surface layer composed of vivianite-like mineral structures covered a large proportion of the glass surface (Fig. 11), in agreement with PHREEQC modelling of solution data, and suggesting

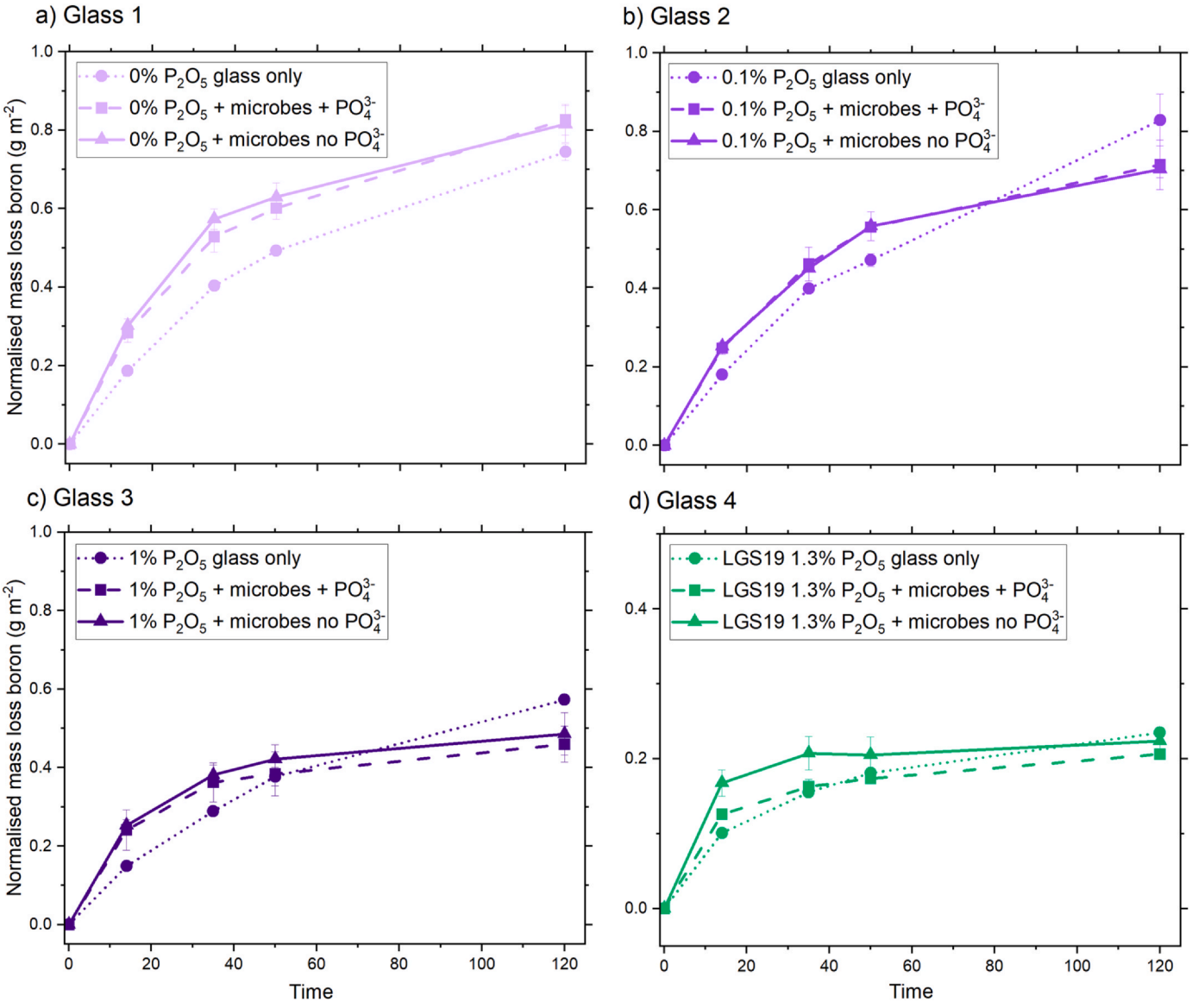

Fig. 10. Normalized mass loss of boron for borosilicate glasses 1–4 in the SO_4^{2-} reducing system where glucose was added as the electron donor. Error bars are the standard deviation of triplicate measurements. Note the different normalised mass loss scale for glass 4 (LAW LGS19).

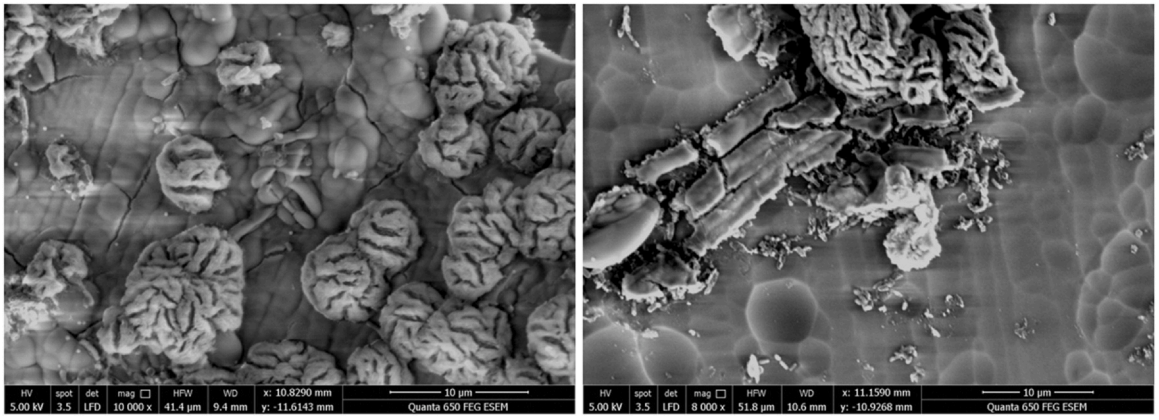

Fig. 11. Mineral precipitation on the surface of altered iron phosphate glasses.

Table 9
Estimated dissolution rates of glass 5, Fe-phosphate glass in oxic media, based on the release of phosphorus into solution. Similar estimates for microbially amended systems were not possible due to the rapid precipitation of Fe(II)-bearing minerals.

System	Time point	Normalised mass loss phosphorus g m^{-2}	Normalised Rate g m^{-2} d^{-1}
Fermentative	168	1.48 ± 0.35	$8.8 \pm 2.0 \times 10^{-3}$
Iron reducing	52	0.65 ± 0.01	$1.3 \pm 0.03 \times 10^{-2}$
Sulphate reducing	120	0.67 ± 0.01	$5.6 \pm 0.8 \times 10^{-3}$

that the system was supersaturated with regard to Fe(II)-phosphate phases (Table 9). It was not possible to calculate an accurate rate of glass dissolution from these samples, due to lack of a conservative tracer. However, PO_4^{3-} release into solution was used to estimate dissolution rates in abiotic systems to be $8.8 \pm 2.0 \times 10^{-3}$, $1.3 \pm 0.03 \times 10^{-2}$, $5.6 \pm 0.8 \times 10^{-3}$ g m^{-2} d^{-1} for fermentative, Fe(III)-reducing and SO_4^{2-}-reducing systems, respectively (Table 9). These rates are likely to be an underestimation as they do not take into account sorption of PO_4^{3-} or precipitation of Fe(III)phosphate phases. It was not possible to estimate the effect of microbial metabolism on the dissolution of iron phosphate glass due to the extensive precipitation of Fe(II)-phosphates, however, the solubilisation of Fe(III) via its reduction to Fe(II) may provide a mechanism by which microbes could accelerate glass dissolution.

4. Conclusions

This study concludes that microbial respiration has the ability to impact the rate of glass dissolution in nuclear waste type glasses and, in return, that glass dissolution can increase microbial metabolism. Phosphorus containing glasses may lead to greater microbial activity at their surfaces by providing a source of the essential macronutrient, phosphorus, and potentially other necessary elements. The effect of increased microbial activity on glass dissolution, however, was modest and dependent on the chemistry of the glass and surrounding environment. This study showed that, whilst breakdown of organics to VFAs lead to an increased rate of glass dissolution in the initial days, the microbial reduction of Fe(III) to Fe(II) caused reduced dissolution rates (presumably by mitigating the detrimental effect of Fe(III) on glass dissolution). This study, although not directly relevant to the metabolic processes likely to occur in a deep geological repository, and perhaps more representative of near surface burial, nevertheless makes useful observations. These experiments show how metabolic processes could exhibit a controlling effect on the near field geochemical conditions of vitrified radioactive waste. The beneficial effect that microbes appear to have on glass durability in the presence of iron is particularly interesting as all waste disposal scenarios involve a high concentration of iron. Exterior iron (initially Fe(0)) will be abundant due to the steel canisters in which most wastes are contained, and a small amount of Fe(III) is likely in vitrified radioactive waste. In a repository, H_2 derived from steel corrosion is expected to drive reduction of any available Fe(III). Although the overall effect of microbial metabolism was to decrease dissolution rates, it was interesting to note that microbial growth was greatest where iron was present in the glass, implying that microbes were able to use glass derived Fe(III) as an electron acceptor. Following on from this study, future work will unpick the complex chemistry of Fe-P interactions within glass alteration layers and explore whether reduction of glass bound Fe(III) has a significant effect on the rate of glass dissolution.

Environmental relevance statement

Vitrified radioactive waste is designed to immobilize long lived radionuclides for time periods up to 106 years until activity has decayed to safe levels. Radioactive elements are chemically incorporated in the glass network and so are released as the glass dissolves. It is, therefore, important to understand the durability of vitrified radioactive waste in subsurface environments to inform the safety case for their long-term disposal. This paper investigates glass-microbe interactions using non-active surrogates for radioactive waste glasses and relevant anaerobic microorganisms to build a mechanistic understanding of glass dissolution in complex natural environments.

CRediT authorship contribution statement

Clare L. Thorpe: Conceptualization, Funding acquisition, Investigation, Methodology, Project administration, Writing – original draft. **Rachel Crawford:** Investigation. **Russell J. Hand:** Writing – review & editing. **Joshua T. Radford:** Investigation. **Claire L. Corkhill:** Writing – review & editing. **Carolyn I. Pearce:** Methodology, Writing – review & editing. **James J. Neeway:** Writing – review & editing. **Andrew E. Plymale:** Methodology, Writing – review & editing. **Katherine Morris:** Writing – review & editing. **Christopher Boothman:** Investigation. **Jonathan R. Lloyd:** Conceptualization, Writing – review & editing.

Data Availability

Data will be made available on request.

Declaration of Competing Interest

The authors declare that they have no known competing financial interests or personal relationships that could have appeared to influence the work reported in this paper.

Acknowledgments

We acknowledge access to the EPSRC RADER National Nuclear User Facility at the University of Manchester, established with the support of EPSRC and BEIS under grant number EP/T011300/1 and the NNUF Programme Management Grant for support to access the laboratories. This research also utilised the HADES/MIDAS and PLEIADES National Nuclear User Facilities at the University of Sheffield, established with financial support from EPSRC and BEIS, under grant numbers EP/T011424/1 and EP/V035215/1. CLC and CLT wish to acknowledge the Engineering and Physical Science Research Council (EPSRC) for fellowship funding under grant awards EP/N017374/1 and EP/S012400/1, respectively. EPSRC is further acknowledged for funding under the Nuclear FiRST Centre for Doctoral Training (EP/G037140/1) and GREEN CDT (EP/S022295/1). JJN, AEP and CIP gratefully acknowledge financial support provided by the U.S. Department of Energy (DOE) Waste Treatment and Immobilization Plant Project at Pacific Northwest National Laboratory (PNNL). PNNL is a multi-program national laboratory operated for DOE by Battelle Memorial Institute operating under Contract No. DE AC05-76RL0-1830. Laser ablation - mass spectrometry was conducted with the assistance of Simon Chenery at the British Geological Survey, Keyworth, UK.

Appendix A. Supporting information

Supplementary data associated with this article can be found in the online version at doi:10.1016/j.jhazmat.2023.132667.

References

[1] ASTM, Standard Test Methods for Determining Chemical Durability of Nuclear, Hazardous, and Mixed Waste Glasses and Multiphase Glass Ceramics: The Product Consistency Test (PCT) (ASTM C1285–21), Book of standards, 12.01, 27 (2021a). DOI:/10.1520/C1285–21.
[2] ASTM, Standard Test Method for Static Leaching of Monolithic Waste Forms for Disposal of Radioactive Waste (ASTM C1220–17), Book of standards, 12.01, 22 (2021b). DOI: /10.1520/C1220–17

[3] Arena H, Godon N, Rebiscoul D, Frugier P, Podor R, Garces R, et al. Impact of iron and magnesium on glass alteration: characterization of the secondary phases and determination of their solubility constants. Appl Geochem 2017;82:119–33. https://doi.org/10.1016/j.apgeochem.2017.04.010

[4] Arena H, Godon N, Rebiscoul D, Podor R, Garces R, Cabie M, et al. Impact of Zn, Mg, Ni and Co elements on glass alteration: additive effects. J Nucl Mater 2016;470:55–67. https://doi.org/10.1016/j.jnucmat.2015.11.050

[5] Bachelet M, Crovisier J, Stille P, Boutin R, Vuilleumier S, Geoffroy V. Biodegradation of the French reference nuclear glass SON 68 by Acidithiobacillus thiooxidans: protective effect of the biofilm, U and REE retention. American Geophysical Union, Fall Meeting; 2008. p. 2008.

[6] Bachelet, M., Crovisier J.L., Stille, P., Vuilleumier, S. and Geoffroy, V. Biological effect of Acidithiobacillus thiooxidans on some potentially toxic elements during alteration of SON 68 nuclear glass. EGU General Assembly 2009, held 19–24 April, 2009 in Vienna,

[7] Backhouse DJ, Corkhill CL, Hyatt NC, Hand RJ. Investigation of the role of Mg and Ca in the structure and durability of aluminoborosilicate glass. (DOI: /). J Non Cryst Solids 2019;512:41–52. https://doi.org/10.1016/j.jnoncrysol.2019.03.003

[8] Bagwell CE, Bhat S, Hawkins GM, Smith BW, Biswas T, Hoover TR, et al. Survival in nuclear waste, extreme resistance, and potential applications gleaned from the genome sequence of kineococcus radiotolerans SRS30216. (DOI: /). PLoS ONE 2008;3(12):e3878https://doi.org/10.1371/journal.pone.0003878

[9] Bassil NM, Bryan N, Lloyd JR. Microbial degradation of isosaccharinic acid at high pH. The. (DOI: /). ISME J 2015;9:310–20. https://doi.org/10.1038/ismej.2014.125

[10] Bennett PC. Quartz dissolution in organic rich aqueous systems. (DOI: /). Geochim Et Cosmochim Acta 1991;55:1781–97. https://doi.org/10.1016/0016-7037(91)90023-X

[11] Bennett PC, Rogers JR, Choi WJ, Hiebert FK. Silicates, silicate weathering, and microbial ecology. (DOI: /). Geomicrobiol J 2001;18(1):3–19. https://doi.org/10.1080/01490450151079734

[12] Bokulich NA, Kaehler BD, Rideout JR, Dillon M, Bolyen E, Knight R, et al. Optimizing taxonomic classification of marker-gene amplicon sequences with QIIME 2's q2-feature-classifier plugin. (DOI: /). Microbiome 2018;6(1):90. https://doi.org/10.1186/s40168-018-0470-z

[13] Boulos L, Prevost M, Barbeau B, Coallier J, Desjardins R. LIVE/DEAD BacLight™: application of a new rapid staining method for direct enumeration of viable and total bacteria in drinking water. J Microbiol Methods 1999;37:77–86. https://doi.org/10.1016/s0167-7012(99)00048-2

[14] Bolyen E, Rideout JR, Dillon MR, Bokulich NA, Abnet CC, Al-Ghalith GA, et al. Reproducible, interactive, scalable and extensible microbiome data science using QIIME 2. (DOI: /). Nat Biotechnol 2019;37:852–7. https://doi.org/10.1038/s41587-019-0209-9

[15] Byrd N, Lloyd JR, Small JS, Taylor F, Bagshaw H, Boothman, et al. Microbial degradation of citric acid in low level radioactive waste disposal: impact on biomineralization reactions. Front Microbiol 2021;12:565855https://doi.org/10.3389/fmicb.2021.565855

[16] Caporaso JG, Lauber CL, Walters WA, Berg-Lyons D, Lozupone CA, Turnbaugh PJ, et al. Global patterns of 16S rRNA diversity at a depth of millions of sequences per sample. (DOI: /). Proc Natl Acad Sci 2011;108(Supplement 1):4516–22. https://doi.org/10.1073/pnas.1000080107

[17] Caporaso JG, Lauber CL, Walters WA, Berg-Lyons D, Huntley J, Fierer N, et al. Ultra-high-throughput microbial community analysis on the Illumina HiSeq and MiSeq platforms. (DOI: /). ISME J 2012;6(8):1621–4. https://doi.org/10.1038/ismej.2012.8

[18] Chapelle FH, O'Neill K, Bradley PM, Methe BA, Ciufo SA, Knobel LL, et al. A hydrogen-based subsurface microbial community dominated by methanogens. Nature 2002;415:312–5. https://doi.org/10.1038/415312a

[19] Chapman NA. Who might be interested in a deep borehole disposal facility for their radioactive waste. (DOI: /). Energies 2019;12(8):1542. https://doi.org/10.3390/en12081542

[20] Chivian D, Brodie EL, Alm EJ, Culley DE, Dehal PS, Desantis TZ, et al. Environmental genomics reveals a single-species ecosystem deep within earth. Science 2008;322(5899):275–8. https://doi.org/10.1126/science.1155495

[21] Crum J, Kissinger R, Cooley S, Silverstein J, Vienna J, Kim D-S, et al. Low-activity waste glass standards preparation and characterization for calibration of analytical instruments PNNL-31372 pacific northwest national laboratory. (DOI: /). Richland, WA, USA2021. https://doi.org/10.2172/1810475

[22] Demetriou A, Pashalidis I. Adsoption of boron on iron-oxide in aqueous solutions. Desalin Water Treat 2012;37:315–20. 10/5004/dwt.2012.2957.

[23] Edwards KJ, Becker K, Colwell F. The deep, dark energy biosphere: Intraterrestrial life on Earth. Annu Rev Earth Planet Sci 2012;40:551–68. https://doi.org/10.1146/ANNUREV-EARTH-042711-105500

[24] Fanciulli M, Bonera E, Carollo E, Zanotti L. EPR and UV-Raman study of BPSG thin films: structure and defects. Microelectron Eng 2001;55(1–4):65–71. https://doi.org/10.1016/S0167-9317(00)00430-5

[25] Francisco P, C M, Mitsui S, Ishidera T, Tachi Y, Doi R, et al. Interaction of FeII and Si under anoxic and reducing conditions: structural characteristics of ferrous iron silicate co-precipitates. Geochim Et Cosmochim Acta 2020;270:1–20. https://doi.org/10.1016/j.gca.2019.11.009

[26] Galai L, Marchetti L, Godon N, Remazeilles C, Refait P. Kinetic study of Fe silicates formation during iron corrosion in deaerated and alkaline si-containing solutions at 50°C. Corros Sci 2023;211:110846https://doi.org/10.1016/j.corsci.2022.110846

[27] García-Balboa C, Chion Bedoya I, González F, Blázquez ML, Muñoz JA, Ballester A. Bio-reduction of Fe(III) ores using three pure strains of Aeromonas hydophila, Serratia feonticola and clostridium celerecrescens and a natural consortium. Bioresour Technol 2010;101(20):7864–71. https://doi.org/10.1016/j.biortech.2010.05.015

[28] Gilbert PUPA, Abrecht M, Frazer BH. The organic-mineral interface in biominerals. Rev Mineral Geochem 2005;59:157–85. https://doi.org/10.2138/rmg.2005.59.7

[29] Gin S, Jegou C, Vernz E. Use of orthophosphate complexing agents to investigate mechanisms limiting the alteration kinetics of French SON 68 nuclear glass. (DOI: /). Appl Geochem 2000;15:1505–25. https://doi.org/10.1016/S0883-2927(00)00013-5

[30] Gin, S., Delaye, J.M., Angeli, F. and Schuller, S. Aqueous alteration of silicate glass: state of knowledge and perspectives. npj Mater Degrad, 5, 42 (2021). DOI: /10.1038/s41529–021-00190–5.

[31] Hendrich S, Johnson B. Aerobic and anaerobic oxidation of hydrogen by acidophilic bacteria. FEMS Microbiol Lett 2013;349:40–5. https://doi.org/10.1111/1574-6968.12290

[32] Humphreys, P., West, J.M. and Metcalfe, R. Microbial Effects on Repository Performance. Technical Report. UK NDA, UK (2010).

[33] Ihira A, Sakamoto T, Saitoh A, Takebe H. Formation of reaction layer and dissolution behaviour of alkali and alkaline-earth iron phosphate glasses in water. (DOI: /). Mater Trans 2020;61(9):1842–7. https://doi.org/10.2320/matertrans.MT-M2020135

[34] Inagaki F, Hinrichs K-U, Kubo Y, Bowles MW, Heuer VB, Hong W-L, et al. Exploring deep microbial life in coal-bearing sediment down to ~2.5 km below the ocean floor. Science 2015;349:420–4. https://doi.org/10.1126/science.aaa6882

[35] Jolley K, Smith R. Iron phosphate glasses: structure determination and radiation tolerance. (DOI: /). Nucl Instrum Methods Phys Res Sect B: beam Interact Mater At 2016;374:8–13. https://doi.org/10.1016/j.nimb.2015.09.043

[36] Jorgensen BB. Shrinking majority of the deep biosphere. (DOI: /). Proc Natl Acad Sci USA 2012;109:15976–7. https://doi.org/10.1073/pnas.121363910

[37] Jorgensen BB, Boetius A. Feast and famine – microbial life in the deep-sea bed. (DOI: /). Nat Rev Microbiol 2007;5:770–81. https://doi.org/10.1038/nrmicro1745

[38] Jorgensen BB, D'Hondt S. Ecology. A starving majority deep beneath the seafloor. Science 2006;314:932–4. https://doi.org/10.1126/science.1133796

[39] Joseph K, Stennett MC, Hyatt NC, Asuvathraman R, Dube CL, Gandy AS, et al. Iron phosphate glasses: bulk properties and atomic scale structure. (DOI: /). J Nucl Mater 2017;494:342–53. https://doi.org/10.1016/j.jnucmat.2017.07.015

[40] Kim C-W, Day DE. Immobilization of Hanford LAW in iron phosphate glasses. (DOI: /). J Non-Cryst Solids 2003;331:20–31. https://doi.org/10.1016/j.jnoncrysol.2003.08.070

[41] Kozich JJ, Westcott SL, Baxter NT, Highlander SK, Schloss PD. Development of a dual-index sequencing strategy and curation pipeline for analyzing amplicon sequence data on the MiSeq illumina sequencing platform. Appl Environ Microbiol 2013;79(17):5112–20. https://doi.org/10.1128/AEM.01043-13

[42] Kooli WM, Junier T, Shakya M, Monachon M, Davenport KW, Vaideeswaran K, et al. Remidial treatment of corroded iron objects by environmental aeromonas isolates. Appl Environ Microbiol 2019;85:3. https://doi.org/10.1128/AEM.02042-18

[43] Kristjansson JK, Stetter KO. Thermophilic Bacteria. CRC Press; 1998. https://doi.org/10.1201/9781003068334

[44] Kuippers G, Boothman C, Bagshaw H, Beard R, Bryan ND, Lloyd JR. Microbial reduction of Fe(III) coupled to the biodegradation of isosaccharinic acid (ISA. Appl Geochem 2019;109:104399https://doi.org/10.1016/j.apgeochem.2019.104399

[45] Kuippers G, Bassil NM, Lloyd JR. Microbial colonization of cementitious geodisposal facilities, and potential "biobarrier" formation. In: Lloyd JR, Cherkouk A, editors. "The Microbiology of Nuclear Waste Disposal" Amsterdam, Netherlands: Elsevier; 2020. p. 157–92. https://doi.org/10.1016/B978-0-12-818695-4.00008-3

[46] Kutvonen H, Rajala P, Carpén L, Bomberg M. Nitrate and ammonia as nitrogen sources for deep subsurface microorganisms. Front Microbiol 2015;6. https://doi.org/10.3389/fmicb.2015.01079

[47] Libert M, Bildstein O, Esnault M, Jullien M, Sellier R. Molecular hydrogen: an abundant energy source for bacterial activity in nuclear waste repositories. (DOI: /). Phys Chem Earth 2011;36:1616–23. https://doi.org/10.1016/j.pce.2011.10.010

[48] Liu SV, Zhou J, Zhang C, Cole DR, Gajdarzicka-Josifovska M, Phelps TJ. Thermophilic Fe(III)-reducing bacteria from the deep subsurface: the evolutionary implications. Science 1997;277(5329):1106–9. https://doi.org/10.1126/science.277.5329.1106

[49] Lloyd JR, Cherkouk A. The Microbiology of Nuclear Waste Disposal. Elsevier; 2020. https://doi.org/10.1016/C2018-0-00298-4

[50] Love K, George J, Bell A, Sweeney F, Cutforth D, Lonegan C, et al. The effects of phosphorus pentoxide additions on the thermal, rheological and structural properties of sodium borosilicate glass. (DOI: /). J Non-Cryst Solids 2023;600:121999https://doi.org/10.1016/j.jnoncrysol.2022.121999

[51] Lovley DR, Phillips EJP. Availability of ferric iron for microbial reduction in bottom sediments of the freshwater tidal Potomac river. Appl Environ Microbiol 1986;52:4. https://doi.org/10.1128/aem.52.4.751-757.1986

[52] Lytle DA, Snoeyink VL. Effect of ortho-and pholyphosphates on the properties of iron particles and suspensions. (DOI: /). J AWWA 2002;94(10):87–99. https://doi.org/10.1002/j.1551-8833.2002.tb09560.x

[53] Mason OU, Nakagawa T, Rosner M, Van Nostrand JD, Zhou J, Maruyama A, et al. First investigation of the microbiology of the deepest layer of ocean crust. (DOI: /). PLoS ONE 2010;5:e15399https://doi.org/10.1371/journal.pone.0015399

[54] McDonald D, Clemente JC, Kuczynski J, Rideout JR, Stombaugh J, Wendel D, et al. The biological observation matrix (BIOM) format or: how I learned to stop worrying and love the ome-ome. Gigascience 2012;1:7. https://doi.org/10.1186/2047-217X-1-7

[55] Mellor E. Lichens and their action on the glass and leadings of church windows. Nature 1923;112:299–300. https://doi.org/10.1038/112299a0
[56] Morita RY. Is H2 the universal energy source for long-term survival? Microb Ecol 2000;38:307–20. https://doi.org/10.1007/s002489901002
[57] Moreira R, Schutz MK, Libert M, Tribollet B, Vivier V. Influence of hydrogen-oxidizing bacteria on the corrosion of low carbon steel: local electrochemical investigations. (DOI: /). Bioelectrochemistry 2014;97:69–75. https://doi.org/10.1016/j.bioelechem.2013.10.003
[58] Motamedi M, Karland O, Pedersen K. Survival of sulfate reducing bacteria at different water activities in compacted bentonite. FEMS Microbiol Lett 1996;141(1):83–7. https://doi.org/10.1111/j.1574-6968.1996.tb08367.x
[59] Moser DP, Gihring TM, Brockman FJ, Fredrickson JK, Balkwill DL, Dollhopf ME, et al. Desulfotomaculum and Methanobacterium spp. dominate a 4- to 5-kilometer-deep fault. (DOI: /). Appl Environ Microbiol 2005;71(12):8773–83. https://doi.org/10.1128/AEM.71.12.8773-8783.2005
[60] Munoz F, Montagne L, Delevoye L, Duran A, Pascual L, Cristol S, et al. Phosphate speciation in sodium borosilicate glasses studied by nuclear magnetic resonance. (DOI: /). J Non-Cryst Solids 2006;352:2958–68. https://doi.org/10.1016/j.jnoncrysol.2006.04.016
[61] Onstott TC, Moser DP, Pfiffner SM, Fredrickson JK, Brockman FJ, Phelps TJ, et al. Indigenous and contaminant microbes in ultradeep mines. Environ Microbiol 2003;5:1168–91. https://doi.org/10.1046/j.1462-2920.2003.00512.x
[62] Parkes RJ, Webster G, Cragg BA, Weightman AJ, Newberry CJ, Ferdelman TG, et al. Deep sub-seafloor prokaryotes stimulated at interfaces over geological time. Nature 2005;436:390–4. https://doi.org/10.1038/nature03796
[63] Perez A, Rossano S, Trcera N, Huguenot D, Fourdrin C, Verney-Caron A, et al. Bioalteration of synthetic Fe(III)-, Fe(II)-bearing basaltic glasses and Fe-free glass in the presence of the heterotrophic bacteria strain Pseudomonas aeruginosa: Impact of siderophores. (DOI: /). Geochmica Et Cosmochim Acta 2016;188:147–62. https://doi.org/10.1016/j.gca.2016.05.028
[64] Pedersen K. Investigations of subterranean bacteria in deep crystalline bedrock and their importance for the disposal of nuclear waste. (DOI: /). Can J Microbiol 1996;42:382–91. https://doi.org/10.1139/m96-054
[65] Pedersen K. Microbial life in deep granitic rock. (DOI: /). FEMS Microbiol Rev 1997;20:399–414. https://doi.org/10.1016/S0168-6445(97)00022-3
[66] Pedersen K. Exploration of deep intraterrestrial microbial life: current perspectives. (DOI: /). FEMS Microbiol Lett 2000;185:9–16. https://doi.org/10.1111/j.1574-6968.2000.tb09033.x
[67] Pedregosa F, Grisel O, Weiss R, Passos A, Brucher M, Varoquax G, et al. Scikit-learn: machine learning in python. J Mach Learn Res 2011;12:2825–30.
[68] Poluektov PP, Schmidt OV, Kascheev VA, Ojovan MI. Modelling aqueous corrosion of nuclear waste phosphate glass. (DOI: /). J Nucl Mater 2017;484:357–66. https://doi.org/10.1016/j.jnucmat.2016.10.033
[69] Porder S, Ramachandran S. The phosphorus concentration of common rocks – a potential driver of ecosystem P status. Plant Soil 2013;367:41–55. https://doi.org/10.1007/s11104-012-1490-2
[70] Postgate JR, Kent HM, Robson RL, Chesshyre JA. The genomes of Desulfovibrio gigas and D. vulgaris. Microbiology 1984;130:7. https://doi.org/10.1099/00221287-130-7-1597
[71] Quast C, Pruesse E, Yilmaz P, Gerken J, Schweer T, Yarza P, et al. The SILVA ribosomal RNA gene database project: improved data processing and web-based tools. Nucl Acids Res 2013;41(*D1*):*D590*–6. https://doi.org/10.1093/nar/gks1219
[72] Ravarian R, Moztarzadeh F, Solati Hashjin M, Rabiee SM, Khoshakhlagh P, Tahriri M. Synthesis, characterization and bioactivity investigation of bioglass/hydroxyapatite composite. Ceram Int 2010;36(1):291–7. https://doi.org/10.1016/j.ceramint.2009.09.016
[73] Rong C, Wong-Moon KC, Li H, Hrma P, Cho H, Solid-state NMR. investigation of phosphorus in aluminoborosilicate glasses. (DOI: /). J Non-Cryst Solids 1998;223:32–42. https://doi.org/10.1016/S0022-3093(97)00436-5
[74] Rogers JR, Bennett PC. Mineral stimulation of subsurface microorganisms: release of limiting nutrients from silicates. (DOI: /). Chem Geol 2004;203:91–108. https://doi.org/10.1016/j.chemgeo.2003.09.001
[75] Roussel EG, Bonavita MA, Querellou J, Cragg BA, Webster G, Prieur D, et al. Extending the sub-sea-floor biosphere. Science 2008;320:1046. https://doi.org/10.1126/science.1154545
[76] Ruiz-Fresneda MA, Martinez-Moreno MF, Provedano-Priego C, Morales-Hidalgo M, Jroundi F, Merroun ML. Impact of microbial processes on the safety of deep geological repositories for radioactive waste. Front Microbiol 2023;14. https://doi.org/10.3389/fmicb.2023.1134078
[77] Santos FA, Silva AC, Santos C, Simba BG, Bartolomé JF, Duran T, et al. Biocide glass based on Nb2O5-SiO-CaO-Na2O system. (DOI: /). Mater Lett 2016;183:277–80. https://doi.org/10.1016/j.matlet.2016.07.117
[78] Sassoni E. Hydroxyapatite and other calcium phosphates for the conservation of cultural heritage: a review. (DOI: /). Materials 2018;11(4):557. https://doi.org/10.3390/ma11040557
[79] Shukla M, Chaturvedi R, Tamhane D, Vyas P, Archana G, Apte S, et al. Multiple-stress tolerance of ionizing radiation-resistant bacterial isolates obtained from various habitats: correlation between stresses. Curr Microbiol 2007;54:142–8. https://doi.org/10.1007/s00284-006-0311-3
[80] Smith SL, Rizoulis A, West JM, Lloyd JR. The Microbiology of a hyper-alkaline spring, and impacts of an alkali-tolerant community during sandstone batch and column experiments representative of a geological disposal facility for intermediate-level radioactive waste. (DOI: /). Geomicrobiol J 2016;33(6):455–67. https://doi.org/10.1080/01490451.2015.1049677
[81] Stranghoener M, Schippers A, Dultz S, Behrens H. Experimental Microbial Alteration and Fe Mobilization From Basaltic Rocks of the ICDP HSDP2 Drill Core, Hilo, Hawaii. Front Microbiol 2018;9. https://doi.org/10.3389/fmicb.2018.01252
[82] Strachan D. Glass dissolution as a function of pH and temperature and the implications for mechanism and experiments. Geochim Et Cosmochim Acta 2017;219:111–23. https://doi.org/10.1016/j.gca.2017.09.008
[83] Stookey LL. Ferrozine-a new spectrophotometric reagent for iron. (DOI: /). Anal Chem 1970;42(7):779–81. https://doi.org/10.1021/ac60289a016
[84] Techer I, Advocat T, Lancelot J, Liotard J-M. Basaltic glass: alteration mechanisms and analogy with nuclear waste glasses. J Nucl Mater 2000;282(1):40–6. https://doi.org/10.1016/S0022-3115(00)00399-8
[85] Teske AP. The deep subsurface biosphere is alive and well. Trends Microbiol 2005;13:402–4. https://doi.org/10.1016/j.tim.2005.07.004
[86] Thorpe CL, Neeway JJ, Pearce CI, Hand RJ, Fisher AJ, Walling SA, et al. Forty years of durability assessment of nuclear waste glass by standard methods. NPJ Mater Degrad 2021;5:51. https://doi.org/10.1038/s41529-021-00210-4
[87] Thorpe CL, Boothman C, Lloyd JR, Law GTW, Bryan ND, Atherton N, et al. The interactions of strontium and technetium with Fe(II) bearing biominerals: implications for bioremediation of radioactively contaminated land. Appl Geochem 2014;40:135–43. https://doi.org/10.1016/j.apgeochem.2013.11.005
[88] Uluisik I, Karakaya HC, Koc A. The importance of boron in biological systems. J Trace Elem Med Biol 2018;45:156–62. https://doi.org/10.1016/j.jtemb.2017.10.008
[89] Uroz S, Calvaruso, Turpault M-P, Frey-Klett P. Mineral weathering by bacteria: ecology, actors and mechanisms. Trends Microbiol 2009;17(8):378–87. https://doi.org/10.1016/j.tim.2009.05.004
[90] Valbi V, Leplat J, François A, Perez A, Trichereau B, Ranchoux C, et al. Bacterial diversity on stained glass windows. Int Biodeterior Biodegrad 2023;177:105529https://doi.org/10.1016/j.ibiod.2022.105529
[91] Vargas KGK, Qi Z. P immobilizing materials for lake internal loading control: a review towards future developments. Crit Rev Environ Sci Technol 2019;49(6):518–52. https://doi.org/10.1080/10643389.2018.1551300
[92] Ventura BA, González F, Ballester A, Blázquez ML, Muñoz JA. Bioreduction of iron compounds by Aeromonas hydrophila. (DOI: /). Int Biodeterior Biordegrad. 2015;103:69–76. https://doi.org/10.1016/j.ibiod.2015.03.034
[93] Weaver JL, DePriest, Plymale AE, Pearce CI, Arey B, Koestler RJ. Microbial interactions with silicate glasses. npj Mater Degrad 2021;5:11. https://doi.org/10.1038/s41529-021-00153-w
[94] White DC, Phelps TJ, Onstott TC. What's up down there? Curr Opin Microbiol 1998;1:286–90. https://doi.org/10.1016/s1369-5274(98)80031-3